

Phase I/II trial of iPS-cell-derived dopaminergic cells for Parkinson's disease

<https://doi.org/10.1038/s41586-025-08700-0>

Received: 9 August 2024

Accepted: 24 January 2025

Published online: 16 April 2025

Open access

 Check for updates

Nobukatsu Sawamoto^{1,8}, Daisuke Doi^{2,8}, Etsuro Nakanishi^{1,8}, Masanori Sawamura^{1,8}, Takayuki Kikuchi³, Hodaka Yamakado¹, Yosuke Taruno¹, Atsushi Shima¹, Yasutaka Fushimi⁴, Tomohisa Okada⁴, Tetsuhiro Kikuchi², Asuka Morizane², Satoe Hiramatsu², Takayuki Anazawa⁵, Takero Shindo⁶, Kentaro Ueno⁷, Satoshi Morita⁷, Yoshiki Arakawa³, Yuji Nakamoto⁴, Susumu Miyamoto³, Ryosuke Takahashi¹✉ & Jun Takahashi²✉

Parkinson's disease is caused by the loss of dopamine neurons, causing motor symptoms. Initial cell therapies using fetal tissues showed promise but had complications and ethical concerns^{1–5}. Pluripotent stem (PS) cells emerged as a promising alternative for developing safe and effective treatments⁶. In this phase I/II trial at Kyoto University Hospital, seven patients (ages 50–69) received bilateral transplantation of dopaminergic progenitors derived from induced PS (iPS) cells. Primary outcomes focused on safety and adverse events, while secondary outcomes assessed motor symptom changes and dopamine production for 24 months. There were no serious adverse events, with 73 mild to moderate events. Patients' anti-parkinsonian medication doses were maintained unless therapeutic adjustments were required, resulting in increased dyskinesia. Magnetic resonance imaging showed no graft overgrowth. Among six patients subjected to efficacy evaluation, four showed improvements in the Movement Disorder Society Unified Parkinson's Disease Rating Scale part III OFF score, and five showed improvements in the ON scores. The average changes of all six patients were 9.5 (20.4%) and 4.3 points (35.7%) for the OFF and ON scores, respectively. Hoehn–Yahr stages improved in four patients. Fluorine-18-L-dihydroxyphenylalanine (¹⁸F-DOPA) influx rate constant (K_i) values in the putamen increased by 44.7%, with higher increases in the high-dose group. Other measures showed minimal changes. This trial (jRCT2090220384) demonstrated that allogeneic iPS-cell-derived dopaminergic progenitors survived, produced dopamine and did not form tumours, therefore suggesting safety and potential clinical benefits for Parkinson's disease.

Parkinson's disease (PD) is characterized by the loss of dopamine (DA) neurons in the substantia nigra, leading to a motor syndrome characterized by bradykinesia, rigidity and resting tremor. Medical treatment effectively alleviates PD symptoms in the early stages, but chronic use results in complications such as motor fluctuations and drug-induced dyskinesias. Consequently, cell therapies to replace lost DA neurons have been investigated as an alternative treatment.

Initial open-label studies demonstrated that human fetal ventral mesencephalon (hfVM) engrafted to the host striatum can synthesize DA and improve motor symptoms^{1–3}. However, double-blinded placebo-controlled trials failed to demonstrate substantial efficacy and revealed side effects such as graft-induced dyskinesias (GIDs)^{4,5}. Moreover, ethical issues and difficulties in maintaining a stable supply have hindered the clinical application of hfVM. European researchers are currently conducting a clinical trial to re-evaluate hfVM (NCT01898390)⁷, while PS-cell-derived DA neurons are being explored as an alternative

donor source⁶. Recently, a single compassionate use case of autologous transplantation suggested the potential of iPS cells⁸. Moreover, clinical trials using human embryonic stem cells are also ongoing (NCT04802733⁹ and NCT05635409¹⁰).

We previously developed a method to induce DA neurons from human iPS cells and sort for DA progenitors¹¹. These cells produced DA in the brains of non-human primate PD models and improved their motor symptoms¹². After preclinical studies confirming safety in terms of tumorigenicity, toxicity and biodistribution¹³, we received approval from the Japanese government and the institutional review board of Kyoto University. Here we report the results of our clinical trial launched in 2018.

Participants

Initially, seven patients were enrolled at Kyoto University Hospital and diagnosed according to Movement Disorder Society (MDS) clinical

¹Department of Neurology, Kyoto University Graduate School of Medicine, Kyoto, Japan. ²Department of Clinical Application, Center for iPS Cell Research and Application, Kyoto University, Kyoto, Japan. ³Department of Neurosurgery, Kyoto University Graduate School of Medicine, Kyoto, Japan. ⁴Department of Diagnostic Imaging and Nuclear Medicine, Kyoto University Graduate School of Medicine, Kyoto, Japan. ⁵Department of Surgery, Kyoto University Graduate School of Medicine, Kyoto, Japan. ⁶Department of Hematology/Oncology, Kyoto University Graduate School of Medicine, Kyoto, Japan. ⁷Department of Biomedical Statistics and Bioinformatics, Kyoto University Graduate School of Medicine, Kyoto, Japan. ⁸These authors contributed equally: Nobukatsu Sawamoto, Daisuke Doi, Etsuro Nakanishi, Masanori Sawamura. ✉e-mail: ryosuket@kuhp.kyoto-u.ac.jp; jbtaka@cira.kyoto-u.ac.jp

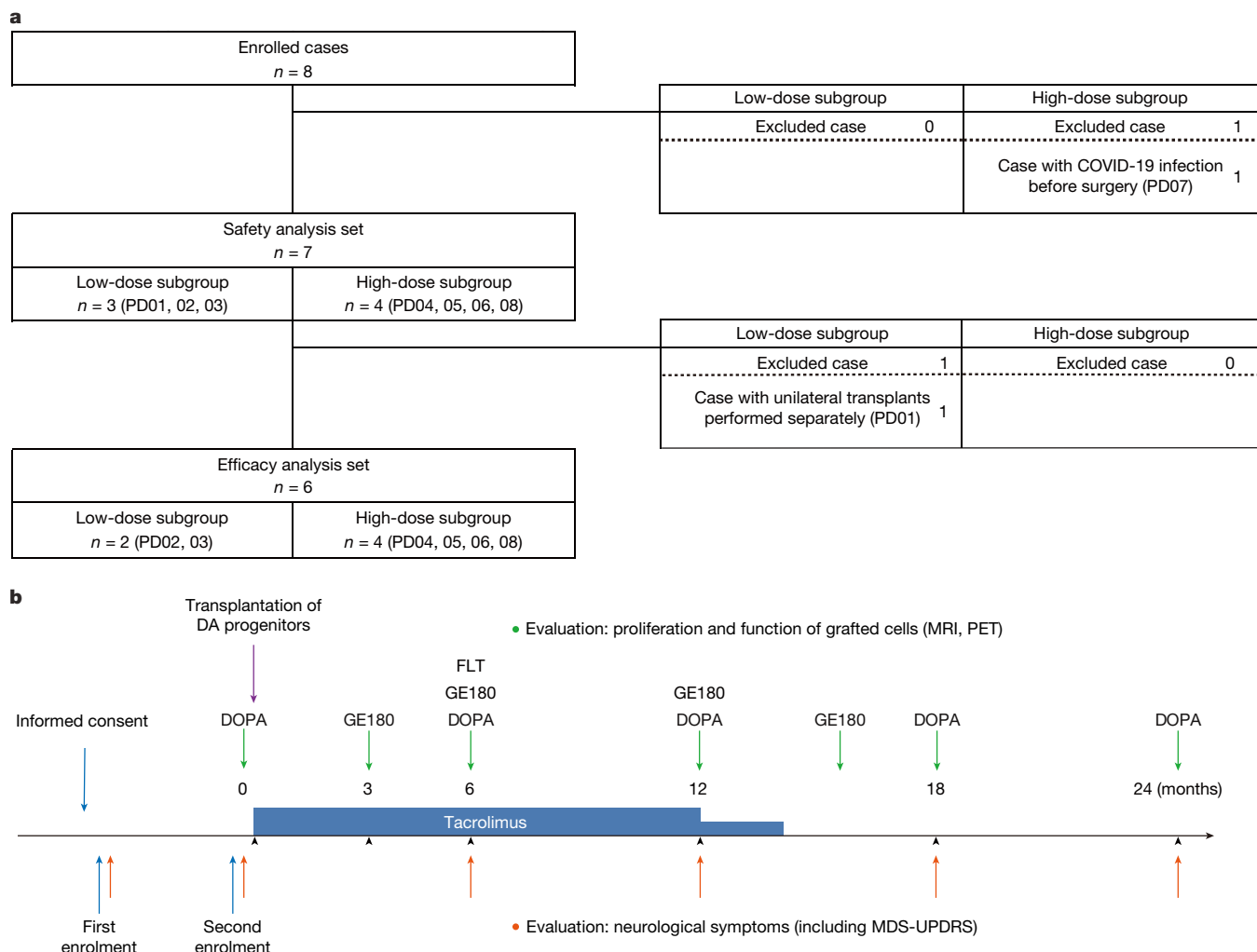


Fig. 1 | Enrolment and follow-up. **a**, Patients were recruited and evaluated at Kyoto University Hospital between August 2018 and January 2019. The first three patients were categorized into the low-dose subgroup, while the remaining four were classified into the high-dose subgroup. One registered patient was excluded before surgery owing to a COVID-19 infection. The first patient received unilateral surgeries with an eight-month interval between procedures and was included only in the safety assessment. Efficacy analysis was conducted on the remaining six patients. **b**, After providing informed consent, the patients were enrolled in this clinical trial and underwent neurological evaluation for more than 6 months. If no notable symptomatic changes were observed during this

period, patients were re-enrolled for surgery and underwent further neurological evaluation (including MDS-UPDRS) and an ¹⁸F-DOPA PET study. After cell transplantation, brain imaging (MRI and PET) and neurological assessments (including MDS-UPDRS) were performed at 3, 6, 12, 18 and 24 months. PET studies included ¹⁸F-DOPA (to assess DA synthesis), ¹⁸F-GE180 (to detect inflammation) and ¹⁸F-FLT (to assess cell proliferation). For immunosuppression, tacrolimus (0.06 mg per kg twice daily) was administered, with the dosage adjusted to maintain target trough levels of 5–10 ng ml⁻¹. The dose was reduced by half at 12 months and discontinued at 15 months.

criteria¹⁴. However, one patient dropped out due to a coronavirus disease 2019 (COVID-19) infection, necessitating the enrolment of an additional patient later. To confirm transplantation safety, the first participant received a left putamen graft and was monitored for 8 months before receiving a right putamen graft. This patient was included only in the safety evaluation. Efficacy was assessed in the remaining six patients who underwent simultaneous bilateral surgery (Fig. 1a,b). All of the patients met the eligibility and exclusion criteria (Supplementary Methods), and their baseline characteristics are summarized in Extended Data Table 1.

Trial design

This investigator-initiated, open-label, phase-I/II, single-centre trial (jRCT2090220384) was conducted at Kyoto University Hospital to investigate the safety and efficacy of striatal transplantation of

allogeneic iPS-cell-derived DA progenitors in patients with PD. The patients underwent bilateral transplantation of DA progenitors and were monitored for 24 months. Three patients (PD01–03) received a low-dose transplant (2.1–2.6 × 10⁶ cells per hemisphere) and four patients (PD04–06 and PD08) received a high-dose transplant (5.3–5.5 × 10⁶ cells per hemisphere) (Fig. 1a). Tacrolimus (0.06 mg per kg twice daily) was administered and adjusted to target trough levels (5–10 ng ml⁻¹), with the dosage reduced by half at 12 months and discontinued at 15 months.

Generation of human iPS cells

The clinical-grade human iPS cell line (QHJ101s04) was established from peripheral blood from a healthy individual homozygous for the most frequent haplotype in the Japanese population (HLA-A 24:02, HLA-B 52:01, HLA-DRB1 15:02, HLA-C 12:02, HLA-DQB1

06:01, HLA-DPB1 09:01), which matches 17% of the Japanese population^{15,16}.

DA progenitor induction and transplant

DA progenitors were induced as previously described¹³. To enrich DA progenitors and eliminate non-target cells, CORIN⁺ (a floor plate marker) cells were sorted on days 11–13, with sorted cells cultured in neural differentiation medium to form aggregate spheres. The fresh final product containing DA progenitors meeting quality-control criteria (Supplementary Table 1) was bilaterally transplanted into the putamen using a neurosurgical navigation system. Single-cell quantitative PCR with reverse transcription (RT-qPCR) analysis confirmed the stable production of DA progenitors. iPS cells differentiated into DA neurons, based on sorting for CORIN⁺ cells, resulting in a final product comprising approximately 60% DA progenitors and 40% DA neurons (Extended Data Fig. 1). Importantly, no TPH2-expressing (a marker for serotonergic neurons) cells were detected. The same donor cells used for patients PDO4–PDO8 were transplanted into rat PD models to evaluate cell survival, proliferation and differentiation potential (Extended Data Fig. 2). Donor cells expressed NURR1 and FOXA2 and, when grafted, differentiated into tyrosine hydroxylase-positive (TH⁺) DA neurons, improving the rotational behaviour of PD model rats. At 24 or 32 weeks after transplantation, no tumour-like overgrowth was observed, and Ki-67⁺ (a marker for proliferating cells) cells were less than 1.0% and sparsely distributed in the grafts. Furthermore, no 5-hydroxytryptamine (5-HT)-positive cells (a marker for serotonergic neurons) were detected.

Primary end point: adverse-event profile

No serious adverse events necessitating hospitalization or resulting in death were reported. All 7 patients (100%) experienced a total of 73 adverse events, comprising 72 mild events and one moderate case of dyskinesia (Supplementary Table 2). The most frequent adverse event was application site pruritus, observed in four patients (57.1%). There were no apparent differences in the spectrum, frequency and severity of treatment-related adverse events between the low-dose and high-dose groups. These events were transient, and most were unlikely related to either cell transplantation or tacrolimus. The single adverse event possibly related to cell transplantation was neck stiffness and painful dystonia in the right upper limb during the drug-on state. Tacrolimus administration was well tolerated but potentially associated with adverse events in three patients (42.9%), including hepatic impairment ($n = 1$), increased gamma-glutamyltransferase levels ($n = 1$), cystitis ($n = 1$), nail dermatophytosis ($n = 1$) and renal impairment ($n = 2$).

Secondary end point: safety

Serial magnetic resonance imaging (MRI) scans during follow-up periods identified the grafts as hyperintense areas in the putamen on T2-weighted images in all of the patients. Quantitative analysis of graft size showed a gradual volume increase over 24 months, with no evidence of tumour-like abnormal enlargement (Extended Data Fig. 3). None of the patients exhibited increased accumulation of fluorine-18-fluorothymidine (¹⁸F-FLT) in the transplanted striatum. Moreover, no patients displayed T2-weighted and fluid-attenuated inversion recovery (FLAIR) hyperintense regions nor appreciable uptake of the translocator protein-ligand, fluorine-18-flutriclamide (¹⁸F-GE180; a marker of microglial activation)¹⁷, indicative of apparent inflammation in the putamen and surrounding areas.

The Unified Dyskinesia Rating Scale (UDysRS) total scores¹⁸ increased at 24 months in all patients, except for PDO6, with an average increase of 12.3 points (116.4%) from the baseline (Extended Data Table 2). Excluding PDO1, who underwent surgery in two stages with an 8-month interval

and was observed for 32 months, the average increase was 12.2 points (81.7%; Fig. 2a,b). In the self-report motor diaries, patients recorded dyskinesia during the on-time period. No apparent increase in troublesome dyskinesia was observed during off-time.

Secondary end point: efficacy

Among the six patients in the efficacy group, four (PDO2, PDO3, PDO4 and PDO8) showed an improvement in motor function during the off-time period (more than 12 h without medication), as assessed by the MDS Unified Parkinson's Disease Rating Scale (MDS-UPDRS)¹⁹ part III. The average change from the baseline was -9.5 points (-20.4%) at 24 months, apparently independent of the dose of transplanted cells (Fig. 2c,d and Extended Data Table 2). Regarding MDS-UPDRS part III ON (with medication), five patients (PDO2, PDO3, PDO4, PDO5 and PDO8) improved, with an average change from the baseline of -4.3 points (-35.7%) at 24 months (Fig. 2e,f and Extended Data Table 2). Whereas MDS-UPDRS part III is based on an objective examination by a neurologist, parts I and II are derived from patient interviews about motor and non-motor functions in daily life. When evaluating the combined MDS-UPDRS parts I + II + III OFF, a mild improvement of -3.1 points (-7.2%) on average was observed at 24 months (Extended Data Table 3).

In our evaluation of the Hoehn–Yahr stage during off-time, four patients improved: PDO2 by 2 stages and PDO3, PDO6 and PDO8 by 1 stage each at 24 months. One patient (PDO3) improved by 1 stage during on-time (Extended Data Fig. 4 and Extended Data Table 2).

Other secondary measures, such as on/off time and the 39-item Parkinson's Disease Questionnaire (PDQ-39), were also analysed. While some patients showed improvement during observations, on average, no apparent improvement was observed at 24 months (Extended Data Fig. 5 and Extended Data Table 2). Throughout the study, patients' anti-parkinsonian medication doses were maintained unless there was a therapeutic necessity. This approach was taken to avoid confounding the assessment of transplantation outcomes, as changes in individualized anti-parkinsonian medication could affect the results. Consequently, the mean levodopa equivalent daily dose (LEDD)^{20,21} remained nearly stable during the trial, with an average increase of 6.15 mg per day (0.65% decrease) at 24 months (Extended Data Fig. 5 and Extended Data Table 2).

The total mean putaminal ¹⁸F-DOPA K_i values increased by 44.7% (from 0.0032 to 0.0043) at 24 months. Specifically, the low-dose group showed a 7.0% increase, whereas the high-dose group exhibited a 63.5% increase (Extended Data Table 2). ¹⁸F-DOPA K_i values increased in two out of the four transplanted putamen in the low-dose group and seven out of the eight transplanted putamen in the high-dose group (Fig. 3a,b,e and Extended Data Fig. 6). By contrast, the total mean caudate nucleus ¹⁸F-DOPA K_i value decreased (Fig. 3c). Consequently, the ratio of K_i values in the putamen to the caudate nucleus increased at 24 months in all cases, suggesting an increase of DA synthesis in the putamen despite pathological deterioration (Fig. 3d).

Discussion

The replacement of lost DA neurons with hfVM in patients with PD began in the 1980s^{22,23}. Although PS cells are expected to be an alternative donor cell source to hfVM, the safety and efficacy of iPS-cell-derived DA progenitors remains unclear. This first clinical trial using iPS cells confirmed that iPS-cell-derived DA progenitors can survive without forming tumours and produce DA in the putamen of patients with PD. Moreover, there were no serious adverse events or GIDs. Four out of six patients showed improvement in MDS-UPDRS part III OFF at 24 months after transplantation, suggesting that grafted cells functioned as DA neurons.

No serious adverse events were reported for all seven patients subjected to safety assessment. The graft size measured with MRI

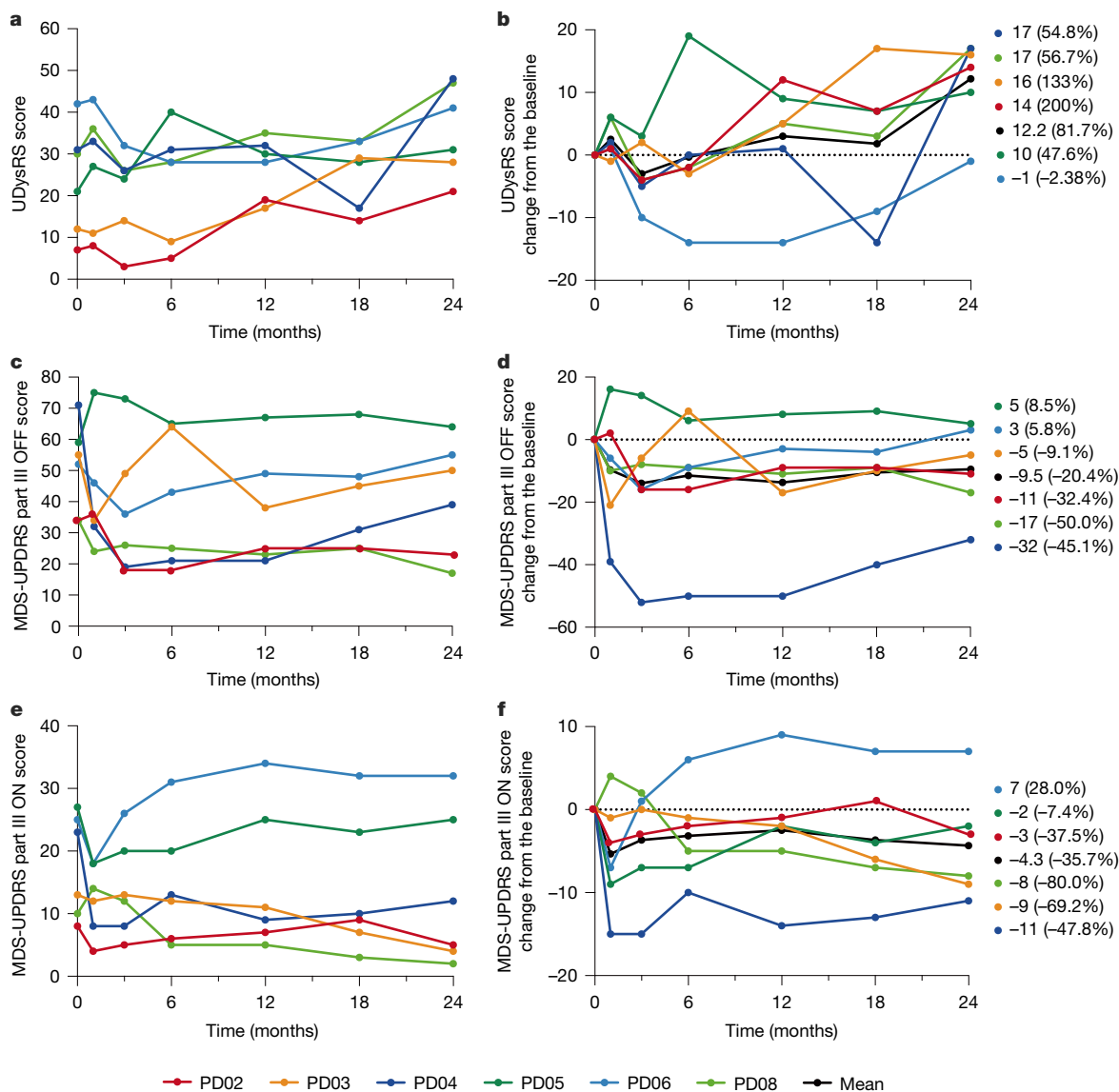


Fig. 2 | Chronological changes in clinical end points. a, b, Chronological changes in the UDysRS scores for each patient from registration (0 months) to the end of the observation period (24 months) for safety assessment. **b,** Score changes from the baseline, with the mean represented by the black line. Absolute and relative (percentage) changes at 24 months are shown on the right. **c–f,** Chronological changes in MDS-UPDRS part III scores during the

medication-off (**c,d**) and medication-on (**e,f**) periods for each patient from registration (0 months) to the end of observation (24 months) for efficacy assessment. **d,f,** Score changes from the baseline. The mean is represented by the black line. The absolute and relative (percentage) changes at 24 months are shown on the right.

T2-weighted images gradually increased over the 24 months. However, no tumorigenic overgrowth was identified, as evidenced by the absence of ¹⁸F-FLT uptake, a marker of cellular proliferation, which was indirectly supported by results from the transplantation experiment using the same donor cells into PD model rats. Histological analyses at 24 or 32 weeks showed no tumour-like overgrowth, with less than 1.0% of cells being Ki-67 positive. Rather than proliferation, a previous animal study reported that the apparent increase in graft volume was due to the spread of the grafted cells⁹. While such effects may also apply to our trial, further confirmation through long-term follow-up and post-mortem histological examinations is necessary. The spectrum of adverse events was similar to those encountered with chronic DA replacement medication, tacrolimus administration and brain surgery. Neck stiffness and painful dystonia in the right upper limb were noted in PD01 during the drug-on state, a phenomenon possibly related to the grafts. Tacrolimus- and surgery-related adverse events were manageable and reversible.

One critical concern about hfVM transplantation was GIDs^{4,5,24}. In this trial, six out of seven patients showed a mild worsening of dyskinesia, resulting in an average increase in the UDysRS total score of 12.3 points (116.4%) from the baseline at 24 months, probably because anti-parkinsonian medication doses were maintained throughout the trial, except when therapeutic adjustments were necessary. The protocol was designed to minimize the impact of medication changes. Consistently, patients recorded dyskinesia in both upper and lower extremities during the on-time period. This clinical presentation is typical for drug-induced dyskinesia and not for GIDs, which occur during the off-time and are often observed predominantly in the lower extremities^{4,5,24}. This suggests that grafted cells replicate the effects of levodopa, including the tendency to induce dyskinesias in susceptible patients. Alternatively, a focal rather than diffuse distribution of DA stimulation from the graft may exacerbate dyskinesia²⁵. In previous reports, GIDs were attributed to serotonergic neurons contained in hfVM tissue^{26–28}. In our DA progenitor preparation, we

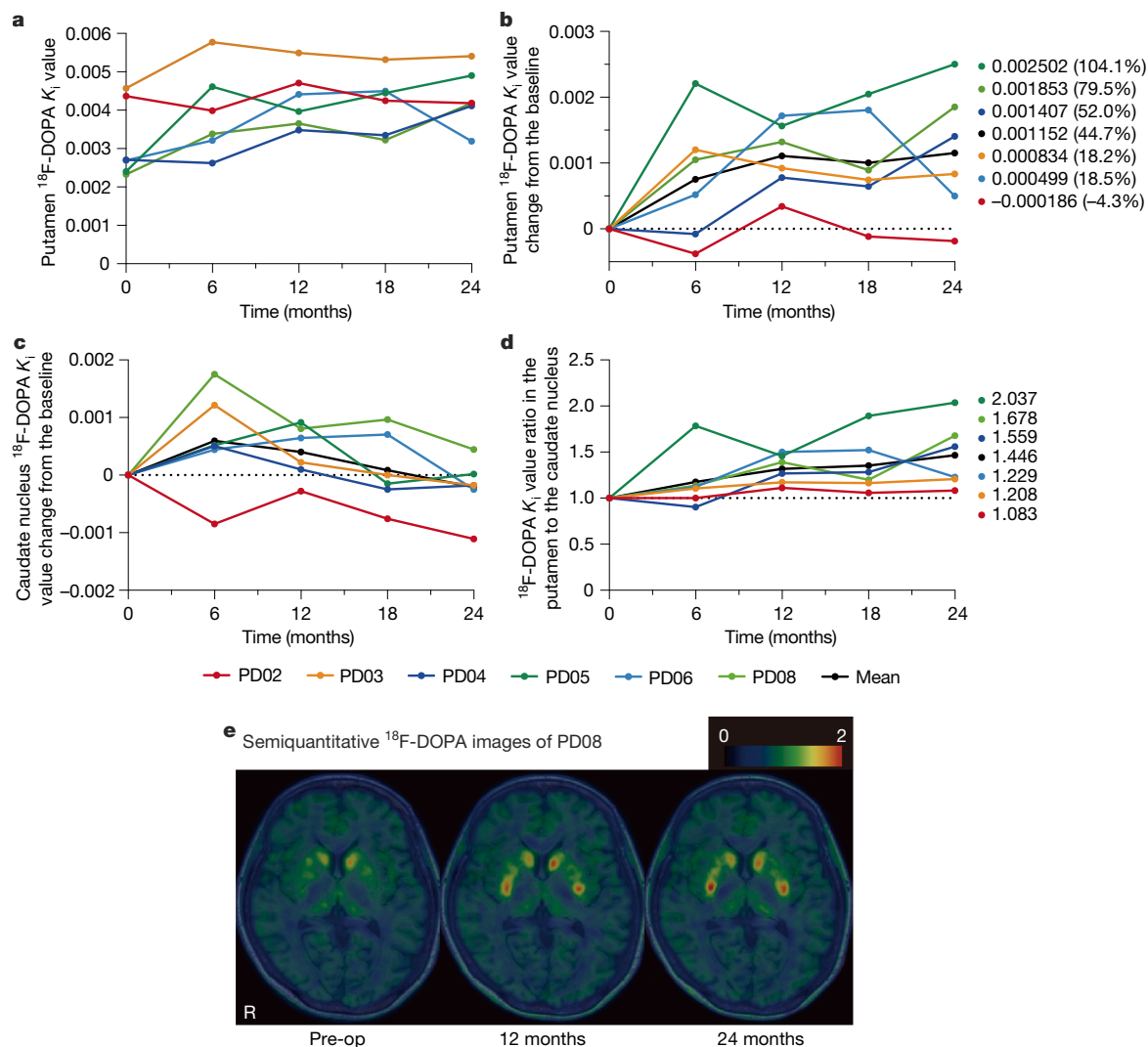


Fig. 3 | DA synthesis detected by ^{18}F -DOPA PET. a, b, Chronological changes in ^{18}F -DOPA K_i values (average of both sides) in the putamen for each patient from registration (0 months) to the end of the observation period (24 months). **b,** The K_i value changes from the baseline; the mean is represented by the black line. The absolute and relative (percentage) changes at 24 months are shown on the right. **c,** The ^{18}F -DOPA K_i value (average of both sides) changes from the baseline in the caudate nucleus for each patient, indicating pathological deterioration in PD. **d,** The ratio of K_i values between the putamen and the

caudate nucleus, highlighting the impact of cell transplantation on pathological deterioration. The percentage changes at 24 months are shown on the right. **e,** Semiquantitative ^{18}F -DOPA images generated at 80–90 min after injection by subtracting the occipital background signal and normalizing the result to the occipital activity in patient PD08. The colour change from dark green to red in the bilateral putamen indicates increased ^{18}F -DOPA uptake, reflecting DA synthesis by grafted cells. Pre-op, pre-operation; R, right.

purified CORIN⁺ medial plate cells and eliminated lateral plate cells, which include serotonergic neurons. As a result, we detected no 5-HT⁺ cells in donor-cell-derived grafts in rat PD models. This purification process may have contributed to the absence of GIDs in our trial.

The appropriate regimen of immunosuppression in allogeneic neural transplantation remains controversial. Previous clinical trials used a different combination of immunosuppressant drugs, including ciclosporin, azathioprine and prednisolone^{4–6,29}. Our previous non-human-primate studies demonstrated no acute immune response after allogeneic transplantation of monkey iPS-cell-derived DA progenitors without immunosuppression³⁰. Furthermore, tacrolimus alone effectively suppressed immune responses during both allotransplantation (monkey to monkey)³¹ and xenotransplantation (human to monkey)¹². On the basis of these findings, we used tacrolimus as the sole immunosuppressant in our clinical trial. Histological analyses from previous fetal cell transplantation studies have shown that grafted DA neurons can survive for 9 to 16 years, even when immunosuppression

is discontinued 6 to 18 months after transplantation^{32,33}. Moreover, our positron-emission tomography (PET) study at 3, 6 and 12 months showed no ^{18}F -GE180 uptake, suggesting the absence of severe inflammation. As a result, we discontinued tacrolimus treatment at 15 months. After terminating immunosuppression, no inflammation due to immune response was observed in the putamen and surrounding areas, as evident by the absence of hyperintensity regions on T2-weighted and FLAIR MRI or increased ^{18}F -GE180 uptake. Moreover, there was no clinical difference between HLA-matched and non-matched patients. However, further confirmation through long-term follow-up and post-mortem histological examinations is necessary for definitive conclusions.

Our results demonstrated a beneficial effect on MDS-UPDRS part III during both on- and off-time periods. Specifically, PD02, PD04 and PD08 showed improvements of 32.4%, 45.1% and 50.0% during off-time at 24 months, respectively, while PD03 showed a 9.1% improvement. Considering the increase in ^{18}F -DOPA uptake, these results suggest that

grafted cells function as DA neurons, therefore functionally replacing lost DA neurons. As this is an open-label trial without a control group, it is important to consider the potential influence of the placebo effect and observer bias. A systematic analysis of placebo responses (placebo effect plus observer bias) in nine double-blind, randomized trials of regenerative therapies for PD reported an average improvement of 4.3 points in MDS-UPDRS part III OFF scores, with a 95% confidence interval of 3.1 to 5.6, with a mean observation time of 11.3 months³⁴. Moreover, a PET study conducted in four out of nine trials showed no significant increase in ¹⁸F-DOPA uptake in sham-operated groups. Furthermore, the placebo effect in patients with PD is thought to be mediated by the release, rather than synthesis, of endogenous DA in the striatum³⁵. On the basis of these findings, at least three patients (PD02, PD04, PD08) in this trial exhibited motor symptom improvements exceeding what could be attributed to placebo responses, potentially due to DA synthesized by the graft. This interpretation should be further validated through post-mortem histological examinations in the future.

Among the three patients (PD02, PD04 and PD08) who exhibited a beneficial effect on MDS-UPDRS part III, only PD02 showed improvement in both the off-time period and PDQ-39 scores. These evaluations are subjective and reflect the patient's perceptions. It is possible that patients had very high expectations for this new treatment, and the results did not meet such high expectations despite objective improvements. In the remaining two patients (PD05 and PD06), motor deficits stabilized at a similar level of decline to those receiving conventional medication^{36,37}. These two patients exhibited a higher degree of deterioration in motor symptoms compared with the other patients during the on-time, suggesting that faster neurodegeneration, especially in the non-dopaminergic systems, diminished the beneficial effects produced by the graft during the trial period. Notably, PD05 was 69 years old at the baseline, and as previous studies on fetal transplants suggest^{4,5}, younger patients with less severe symptoms appear to be more suitable candidates for this treatment. Considering these results, refining patient eligibility criteria may enhance the efficacy of this treatment.

In some cases, especially PD03 and PD06, discrepancies were noted between the MDS-UPDRS part III scores and the Hoehn–Yahr stage. The Hoehn–Yahr stage emphasizes postural instability and mobility issues, whereas the MDS-UPDRS part III offers a more comprehensive evaluation of major motor symptoms in PD. Consequently, improved postural stability and mobility may account for the greater improvement in the Hoehn–Yahr stage compared with changes observed in MDS-UPDRS part III scores of this study.

The substantial increase in putaminal ¹⁸F-DOPA uptake in the high-dose group compared with the low-dose group suggests dose-dependent characteristics. Plots of pre-transplant and post-transplant K_i values and MDS-UPDRS part III OFF scores revealed a mild overall trend but no clear correlation at the individual level (Extended Data Fig. 6i,j). This lack of correlation may be due to the complexity of cell replacement therapy: ¹⁸F-DOPA uptake does not necessarily reflect the activation of postsynaptic neurons, and motor symptoms are influenced by both dopaminergic and non-dopaminergic neural circuits. The functional impact of grafted cells probably requires more than just DA delivery. Successful integration of the graft into the host brain is crucial for achieving meaningful clinical recovery in PD³⁸. Another possibility is that the absolute K_i value is more important than its level of increase and that the number of surviving DA neurons is still insufficient. Previous studies have reported that K_i values of healthy individuals range from 0.010 to 0.017 (with our experience indicating a range of 0.010 to 0.015). While Parkinsonian symptoms typically emerge when K_i values decrease by 41% to 58% from the normal range^{39–41}, even the highest K_i value observed at 24 months fell within the range associated with the onset of initial symptoms. Furthermore, 3 out of 12 putamen samples (PD02R, PD02L, PD06L) did not show an increase in ¹⁸F-DOPA uptake (Extended Data Fig. 6a,b). This may be due

to the technical limitation of measuring uptake in the whole putamen. However, PET images revealed distinct uptake at the injection sites (Extended Data Fig. 6c–h), which may have contributed to symptom improvement. Importantly, there was no difference in adverse events between low- and high-dose groups, and neither graft overgrowth nor GIDs were observed, even in the high-dose group. Considering these results, implanting more cells across a broader area may be necessary to achieve more substantial therapeutic effects. The favourable safety profile observed in this trial provides an opportunity to explore whether a higher dose across a wider region can offer greater clinical efficacy.

Previous open-label trials using human hfVM demonstrated that cells engrafted into the host striatum synthesized DA and improved motor symptoms. In favourable cases, symptom improvement persisted for over 10 years without severe adverse events^{33,42}. While two double-blind, placebo-controlled trials did not find significant differences between the graft and control groups, they did show significant motor symptom improvement in specific subgroups. These findings suggest that cell replacement therapy may be beneficial if appropriate patients are selected. One beneficial subgroup may be patients 60 years old or younger, while another included those with less severe stages (below 50 points as evaluated by the original UPDRS part III OFF score⁴³). Although our results did not fully align with age-related findings, it is notable that the worst case (PD05) was the oldest patient, and the best case (PD08) was the youngest. In terms of MDS-UPDRS part III OFF scores, patients PD02 and PD08, both with scores under 50, demonstrated symptom improvement.

As discussed above, this trial has certain limitations. First, for definitive conclusions regarding the survival of mature DA neurons, inflammation around the graft, and tumorigenicity, post-mortem histological analyses are required. Second, eligibility criteria for optimal patients with PD receiving cell replacement therapy have yet to be defined. Third, graft-derived reinnervation may cover only some DA-depleted striatal regions². These latter factors may partially explain the variable clinical responses observed in this trial. Fourth, this was an open-label trial, susceptible to influence from the placebo effect and physician bias. Future studies should consider a double-blind, placebo-controlled design to minimize these biases. Lastly, the findings of this single-centre, small-sample trial should be confirmed in multi-centre, large-sample trials with appropriate controls.

In conclusion, while the safety and efficacy of iPSC-cell-derived cell products continue to be investigated, this trial demonstrated the safety profile of iPSC-cell-derived DA progenitors. After bilateral putaminal transplantation, the average motor severity was decreased and the mean ¹⁸F-DOPA uptake was increased at the 24-month follow-up. Despite the abovementioned limitations, these findings suggest that allogeneic transplantation of iPSC-cell-derived DA progenitors is a safe and effective regenerative therapy for patients with PD. Future strategies may combine cell transplantation with gene therapy, medication and rehabilitation to enhance efficacy⁴⁴. Moreover, as demonstrated in a single case study⁸, autologous transplantation using iPSC cells may also be a promising option.

Online content

Any methods, additional references, Nature Portfolio reporting summaries, source data, extended data, supplementary information, acknowledgements, peer review information; details of author contributions and competing interests; and statements of data and code availability are available at <https://doi.org/10.1038/s41586-025-08700-0>.

1. Kordower, J. H. et al. Neuropathological evidence of graft survival and striatal reinnervation after the transplantation of fetal mesencephalic tissue in a patient with Parkinson's disease. *N. Engl. J. Med.* **332**, 1118–1124 (1995).
2. Piccini, P. et al. Dopamine release from nigral transplants visualized in vivo in a Parkinson's patient. *Nat. Neurosci.* **2**, 1137–1140 (1999).

3. Barker, R. A., Barrett, J., Mason, S. L. & Bjorklund, A. Fetal dopaminergic transplantation trials and the future of neural grafting in Parkinson's disease. *Lancet Neurol.* **12**, 84–91 (2013).
4. Freed, C. R. et al. Transplantation of embryonic dopamine neurons for severe Parkinson's disease. *N. Engl. J. Med.* **344**, 710–719 (2001).
5. Olanow, C. W. et al. A double-blind controlled trial of bilateral fetal nigral transplantation in Parkinson's disease. *Ann. Neurol.* **54**, 403–414 (2003).
6. Parmar, M., Grealish, S. & Henchcliffe, C. The future of stem cell therapies for Parkinson disease. *Nat. Rev. Neurosci.* **21**, 103–115 (2020).
7. Barker, R. A. & TRANSEURO Consortium. Designing stem-cell-based dopamine cell replacement trials for Parkinson's disease. *Nat. Med.* **25**, 1045–1053 (2019).
8. Schweitzer, J. S. et al. Personalized iPSC-derived dopamine progenitor cells for Parkinson's disease. *N. Engl. J. Med.* **382**, 1926–1932 (2020).
9. Piao, J. et al. Preclinical efficacy and safety of a human embryonic stem cell-derived midbrain dopamine progenitor product, MSK-DA01. *Cell Stem Cell* **28**, 217–229 (2021).
10. Kirkeby, A. et al. Preclinical quality, safety, and efficacy of a human embryonic stem cell-derived product for the treatment of Parkinson's disease, STEM-PD. *Cell Stem Cell* **30**, 1299–1314 (2023).
11. Doi, D. et al. Isolation of human induced pluripotent stem cell-derived dopaminergic progenitors by cell sorting for successful transplantation. *Stem Cell Rep.* **2**, 337–350 (2014).
12. Kikuchi, T. et al. Human iPSC cell-derived dopaminergic neurons function in a primate Parkinson's disease model. *Nature* **548**, 592–596 (2017).
13. Doi, D. et al. Pre-clinical study of induced pluripotent stem cell-derived dopaminergic progenitor cells for Parkinson's disease. *Nat. Commun.* **11**, 3369 (2020).
14. Postuma, R. B. et al. MDS clinical diagnostic criteria for Parkinson's disease. *Mov. Disord.* **30**, 1591–1601 (2015).
15. Okita, K. et al. A more efficient method to generate integration-free human iPSCs. *Nat. Methods* **8**, 409–412 (2011).
16. Yoshida, S. et al. A clinical-grade HLA haplobank of human induced pluripotent stem cells matching approximately 40% of the Japanese population. *Med* **4**, 51–66 (2023).
17. Feeney, C. et al. Kinetic analysis of the translocator protein positron emission tomography ligand [(18)F]JGE-180 in the human brain. *Eur. J. Nucl. Med. Mol. Imaging* **43**, 2201–2210 (2016).
18. Goetz, C. G., Nutt, J. G. & Stebbins, G. T. The unified dyskinesia rating scale: presentation and clinimetric profile. *Mov. Disord.* **23**, 2398–2403 (2008).
19. Goetz, C. G. et al. Movement Disorder Society—sponsored revision of the Unified Parkinson's disease rating scale (MDS-UPDRS): scale presentation and clinimetric testing results. *Mov. Disord.* **23**, 2129–2170 (2008).
20. Tomlinson, C. L. et al. Systematic review of levodopa dose equivalency reporting in Parkinson's disease. *Mov. Disord.* **25**, 2649–2653 (2010).
21. Jost, S. T. et al. Levodopa dose equivalency in Parkinson's disease: updated systematic review and proposals. *Mov. Disord.* **38**, 1236–1252 (2023).
22. Lindvall, O. et al. Human fetal dopamine neurons grafted into the striatum in two patients with severe Parkinson's disease. A detailed account of methodology and a 6-month follow-up. *Arch. Neurol.* **46**, 615–631 (1989).
23. Lindvall, O. et al. Grafts of fetal dopamine neurons survive and improve motor function in Parkinson's disease. *Science* **247**, 574–577 (1990).
24. Hagell, P. et al. Dyskinesias following neural transplantation in Parkinson's disease. *Nat. Neurosci.* **5**, 627–628 (2002).
25. Bankiewicz, K. S. et al. Focal striatal dopamine may potentiate dyskinesias in parkinsonian monkeys. *Exp. Neurol.* **197**, 363–372 (2006).
26. Barker, R. A. & Kuan, W. L. Graft-induced dyskinesias in Parkinson's disease: what is it all about? *Cell Stem Cell* **7**, 148–149 (2010).
27. Politis, M. et al. Serotonergic neurons mediate dyskinesia side effects in Parkinson's patients with neural transplants. *Sci. Transl. Med.* **2**, 38ra46 (2010).
28. Politis, M. et al. Graft-induced dyskinesias in Parkinson's disease: High striatal serotonin/dopamine transporter ratio. *Mov. Disord.* **26**, 1997–2003 (2011).
29. Mendez, I. et al. Simultaneous intra-striatal and intranigral fetal dopaminergic grafts in patients with Parkinson disease: a pilot study. Report of three cases. *J. Neurosurg.* **96**, 589–596 (2002).
30. Morizane, A. et al. Direct comparison of autologous and allogeneic transplantation of iPSC-derived neural cells in the brain of a non-human primate. *Stem Cell Rep.* **1**, 283–292 (2013).
31. Morizane, A. et al. MHC matching improves engraftment of iPSC-derived neurons in non-human primates. *Nat. Commun.* **8**, 385 (2017).
32. Li, J. Y. et al. Lewy bodies in grafted neurons in subjects with Parkinson's disease suggest host-to-graft disease propagation. *Nat. Med.* **14**, 501–503 (2008).
33. Mendez, I. et al. Cell type analysis of functional fetal dopamine cell suspension transplants in the striatum and substantia nigra of patients with Parkinson's disease. *Brain* **128**, 1498–1510 (2005).
34. Polgar, S. et al. The placebo response in double-blind randomised trials evaluating regenerative therapies for Parkinson's disease: a systematic review and meta-analysis. *J. Parkinsons Dis.* **12**, 759–771 (2022).
35. de la Fuente-Fernandez, R. et al. Expectation and dopamine release: mechanism of the placebo effect in Parkinson's disease. *Science* **293**, 1164–1166 (2001).
36. Aviles-Olmos, I. et al. Exenatide and the treatment of patients with Parkinson's disease. *J. Clin. Invest.* **123**, 2730–2736 (2013).
37. Schrag, A. et al. Rate of clinical progression in Parkinson's disease. A prospective study. *Mov. Disord.* **22**, 938–945 (2007).
38. Piccini, P. et al. Delayed recovery of movement-related cortical function in Parkinson's disease after striatal dopaminergic grafts. *Ann. Neurol.* **48**, 689–695 (2000).
39. Pavese, N., Rivero-Bosch, M., Lewis, S. J., Whone, A. L. & Brooks, D. J. Progression of monoaminergic dysfunction in Parkinson's disease: a longitudinal 18F-dopa PET study. *Neuroimage* **56**, 1463–1468 (2011).
40. Khan, N. L. et al. Progression of nigrostriatal dysfunction in a parkin kindred: an [18F]dopa PET and clinical study. *Brain* **125**, 2248–2256 (2002).
41. Nurmi, E. et al. Rate of progression in Parkinson's disease: a 6-[18F]fluoro-L-dopa PET study. *Mov. Disord.* **16**, 608–615 (2001).
42. Kefalopoulou, Z. et al. Long-term clinical outcome of fetal cell transplantation for Parkinson disease: two case reports. *JAMA Neurol.* **71**, 83–87 (2014).
43. Fahn, S., Elton, R. L. & UPDRS Development Committee. in *Recent Developments in Parkinson's Disease* Vol. 2 (eds Fahn, S. et al.) 153–163 (Macmillan, 1987).
44. Takahashi, J. Next steps in regenerative medicine. *Cell Stem Cell* **30**, 509–511 (2023).

Publisher's note Springer Nature remains neutral with regard to jurisdictional claims in published maps and institutional affiliations.



Open Access This article is licensed under a Creative Commons Attribution-NonCommercial-NoDerivatives 4.0 International License, which permits any non-commercial use, sharing, distribution and reproduction in any medium or format, as long as you give appropriate credit to the original author(s) and the source, provide a link to the Creative Commons licence, and indicate if you modified the licensed material. You do not have permission under this licence to share adapted material derived from this article or parts of it. The images or other third party material in this article are included in the article's Creative Commons licence, unless indicated otherwise in a credit line to the material. If material is not included in the article's Creative Commons licence and your intended use is not permitted by statutory regulation or exceeds the permitted use, you will need to obtain permission directly from the copyright holder. To view a copy of this licence, visit <http://creativecommons.org/licenses/by-nc-nd/4.0/>.

© The Author(s) 2025

Methods

Participants

This trial is registered in Japan Registry of Clinical Trials (jRCT) as study number jRCT2090220384 and in University Hospital Medical Information Network (UMIN) as study number UMIN000033564. Patients with PD were diagnosed according to MDS clinical criteria¹⁴. After initial enrolment, all of the patients except for PD01 were observed for more than 6 months and re-enrolled just before surgery. Inclusion criteria included ages 50–69, a disease duration of at least 5 years, Hoehn–Yahr stage 3 or worse during off-time and stage 3 or better during on-time, at least 30% motor improvement with dopaminergic medication (MDS-UPDRS¹⁹ part III) and symptoms unresponsive to current medications (Supplementary Table 3). Exclusion criteria included dementia or psychiatric issues (Supplementary Table 4). A complete list of inclusion and exclusion criteria, along with additional methodological details, is provided in the Supplementary Methods. All of the participants provided written informed consent according to the ethical guidelines of the Kyoto University Hospital Institutional Review Board (K044). Three patients (PD01–03) received a low-dose transplant ($2.1\text{--}2.6 \times 10^6$ cells per hemisphere), and four patients (PD04–06, PD08) received a high-dose transplant ($5.3\text{--}5.5 \times 10^6$ cells per hemisphere) (Fig. 1). The low dose of 5 million cells was selected based on our monkey study¹², which demonstrated both safety and efficacy. After confirming the safety of this dose over one year, the cell count was increased to 10 million. Tacrolimus dosing was adjusted to maintain target trough levels of $5\text{--}10 \text{ ng ml}^{-1}$, reduced by half at 12 months, and discontinued at 15 months. This immunosuppression regimen was based on our non-human primate study¹², in which a single treatment with tacrolimus effectively suppressed immune response during xenotransplantation. Histological examinations from previous fetal cell transplantation cases have shown that grafted DA neurons survived for 9 to 16 years, even with immunosuppression discontinued 6 to 18 months after transplantation. Accordingly, tacrolimus treatment was discontinued at 15 months.

End points and evaluation

Primary end points included the adverse-event profile and graft overgrowth at 24 months ($>3 \text{ cm}^3$ by MRI) (Supplementary Table 5). Secondary outcomes included tumorigenic proliferation, host immune rejection, graft-induced dyskinesia, motor symptom changes (MDS-UPDRS part III) and ^{18}F -DOPA K_i^{45} at 24 months (Supplementary Methods).

Safety was evaluated by documenting adverse events from transplantation to 24 months after operation, coded according to the Medical Dictionary for Regulatory Activities (MedDRA) version 26.1. Dyskinesia severity was assessed using the UDysRS¹⁸. Parkinsonian motor and non-motor symptoms were evaluated using the MDS-UPDRS¹⁹ (parts I–III), the Hoehn–Yahr stages in drug-on and drug-off states and LEDD. Motor diaries, PDQ-39, EuroQoL 5-dimension 5-level (EQ-5D-5L), and the Work Productivity and Activity Impairment questionnaire were used for additional patient-reported outcomes. Tumour-like overgrowth and immune rejection were monitored by MRI, ^{18}F -FLT PET⁴⁶ and ^{18}F -GE180 PET¹⁷. DA neuron survival and differentiation were assessed through motor symptoms and ^{18}F -DOPA PET. These evaluations were scheduled at various intervals after transplantation (Fig. 1b).

Human iPS cells

The clinical-grade human iPS cell line (QHJ101s04) used in this study was previously established from peripheral blood from a healthy individual homozygous for the most frequent haplotype in the Japanese population (HLA-A 24:02, HLA-B 52:01, HLA-DRB1 15:02, HLA-C 12:02, HLA-DQB1 06:01, HLA-DPB1 09:01), which matches 17% of the Japanese population^{15,16}. A master cell bank (MCB) was created, and a single MCB vial was thawed to induce DA progenitors for each patient. Human

iPS cells were maintained with StemFit AK03N media (Ajinomoto) on iMatrix-coated (Matrixome) six-well culture dishes.

DA progenitor induction from human iPS cells

DA progenitors were induced as previously described¹³. Cells for PD01–PD03 were manufactured at Kyoto University, while cells for PD04–PD08 were manufactured at Sumitomo Pharma (international non-proprietary name, raguneprocet). In brief, human iPS cells were seeded at 5.3×10^5 cells per cm^2 onto culture plates coated with laminin 511-E8 fragment (defined as day 0) and cultivated for 11–13 days. To enrich DA progenitors and eliminate non-target cells, CORIN⁺ (a floor plate marker) cells were isolated by a fluorescence-activated cell sorter (BD Influx by BD Bioscience for PD01L, MACSQuant Tyto by Myltenyi Biotec for PD01R–PD03, Gagasort by Cytonome for PD04–PD08) on days 11–13. Sorted CORIN⁺ cells were cultured in 96-well plates with neural differentiation medium to form aggregate spheres until day 30. DA progenitors were induced for each patient individually and prepared as fresh cells on the day of surgery. The final product containing DA progenitors met the quality control criteria (Supplementary Table 1), with cells also analysed by immunostaining and single-cell RT–qPCR (Extended Data Figs. 1 and 2).

Immunostaining

Aggregate spheres were fixed with 4% paraformaldehyde, frozen and sliced at a $10 \mu\text{m}$ thickness. Immunostaining was performed after incubation with an antigen retrieval reagent (LSI Medience) and blocking with 0.3% Triton X-100 and 2% donkey serum for 1 h. Fluorescence images were obtained by using confocal laser microscopes (Fluoview FV1200, Olympus). The antibodies used are described in the ‘Animal experiments’ section below.

Single-cell RT–qPCR analysis

Single-cell cDNA preparation was performed according to the manufacturer's protocol. In brief, a cell suspension of iPS cells (day 0), intermediate cells before sorting (day 13) or the final product (day 30 or 31) at 300 cells per μl were used. The cell suspension was added to C1 suspension reagent (Standard BioTools) at a ratio of 60% for iPS cells or 70% for intermediate cells and DAPs. Then, $6 \mu\text{l}$ of cell suspension and suspension reagent mix, as mentioned above, were loaded onto the C1 Single-Cell Preamp IFC ($10\text{--}17 \mu\text{m}$, Standard BioTools), and the chip was then processed on a Fluidigm C1 instrument using the ‘STA: Cell Load (1782 \times)’ script. After cell loading, visual inspection on an inverted microscope observation was performed to check whether only one living cell was captured in each capture site. Then, the ‘STA: Preamp (1782 \times)’ script, including cell lysis, reverse transcription, and 18 cycle of PCR, was executed. After completion, $3 \mu\text{l}$ of amplified cDNA was mixed with $25 \mu\text{l}$ of C1 DNA dilution reagent (Standard BioTools). Amplified cDNA was used for single-cell RT–qPCR using the Biomark HD System (Standard BioTools), according to the manufacturer's protocol. Gene expression data were analysed and visualized using the Singular Analysis Toolset v.3.6.2 (Standard BioTools). Gene expression patterns were visualized on a t -distributed stochastic neighbour embedding plot. Unsupervised clustering of the cells was performed using the k -means clustering method. The spectrum of gene expression levels in each cell population was visualized by violin plots. DNA primer sequences are listed in Supplementary Table 6.

Cell transplantation

Cells were bilaterally transplanted into the putamen using the iPlan neurosurgical navigation system (BrainLab). Trajectories were designed to target the dorsal and caudal putamen, avoiding sulci and blood vessels. The surgery was performed using the Leksell G frame system (Elekta) and a custom injection needle (TOP). Injection sites were confirmed intraoperatively by cone-beam computed tomography (CT) using the Artis Zeego angiography system (Siemens Healthineers). Three

trajectories per hemisphere were used, with four to eight injections per trajectory, to transplant $2.1\text{--}5.5 \times 10^6$ cells per putamen (Supplementary Table 7 and Supplementary Methods).

Animal experiments

All of the animals were cared for and handled in accordance with the Guidelines for Animal Experiments of Kyoto University and Sumitomo Pharma. Study protocols were approved by the ethical committees of Kyoto University (17-87-7) and Sumitomo Pharma (2014-20). The same donor cells used for patients PD04 (batch, 20022), PD05 (batch, 20048), PD06 (batch, 21004) and PD08 (batch, 21047) were used for transplantation experiments. Fresh day-30 cells (4×10^5 or 5×10^5 cells as the low dose, and 8×10^5 or 10×10^5 cells as the high dose) were injected into the striatum of 6-OHDA-lesioned Parkinsonian nude rats (F344/Njcl-rnu/rnu, CLEA, aged 17–21 weeks). Methamphetamine-induced rotation analyses were conducted at 8 weeks after transplantation and every 4 weeks subsequently. Saline was injected into control rats as a vehicle group in each experiment. Rats are randomly assigned to cell and vehicle group. After 24 to 32 weeks of observation, animals were euthanized with isoflurane and perfused with Ca^{2+} , Mg^{2+} -free PBS, and 4% paraformaldehyde. After immersion in 30% sucrose, the frozen brain slices at 40 μm thickness were prepared for immunohistochemistry. For 3,3'-diaminobenzidine (DAB) staining, brain slices were treated with peroxidase blocking solution (DAKO), incubated sequentially with primary, biotinylated secondary antibodies against rabbit IgG (1:1,000, Vector Laboratories) and avidin-conjugated peroxidase (Vectastain ABC HRP Kit, Vector Laboratories). Signal detection was performed using DAB (DAB Staining Kit, Muto Pure Chemicals) with nickel chloride. Primary antibodies used for immunohistochemistry are as follows: FOXA2 (goat, R&D systems, AF2400, 1:500), NURR1 (mouse, Perseus Proteomics, PP-N1404-00, 1:300), human nucleic antigen (HNA) (mouse, Millipore, MAB1281, 1:500, Ki-67 (rabbit, Abcam, Ab16667, 1:1,000), 5-HT (rat, Millipore MAB352, 1:100) and TH (rabbit, Millipore, AB152, 1:400). Secondary antibodies are as follows: Alexa Fluor 488 anti-Mouse IgG, (donkey, Thermo Fisher Scientific, A21202, 1:400), Alexa Fluor 594 anti-Goat IgG (donkey, Thermo Fisher Scientific, A11058, 1:2,000), Alexa Fluor 594 anti-rabbit IgG (donkey, Thermo Fisher Scientific, A21207, 1:400) and Alexa Fluor 594 anti-rat IgG (donkey, Thermo Fisher Scientific, A21209, 1:400). Images were visualized using a fluorescence microscope (BZ-X710, Keyence) and confocal laser microscopes (LSM880 and LSM800, Zeiss). The number of immunoreactive cells for TH and HNA was quantified in every sixth section throughout the grafts for stereological measurements of the total number of cells per animal⁴⁷.

Statistical analysis

Clinical data were collected by using EDMS-Online (v.3.1, EPS). Safety and efficacy outcomes were summarized using mean values, s.d. values and proportions. Statistical analyses of the clinical data were conducted

using SAS software (v.9.4, SAS Institute). Statistical analyses of animal experiments were performed using GraphPad Prism (v.10.3.1, GraphPad Software).

Reporting summary

Further information on research design is available in the Nature Portfolio Reporting Summary linked to this article.

Data availability

All relevant data from this trial are included in the Article and Supplementary Methods. Source data are provided with this paper.

45. Patlak, C. S. & Blasberg, R. G. Graphical evaluation of blood-to-brain transfer constants from multiple-time uptake data. Generalizations. *J Cereb. Blood Flow Metab.* **5**, 584–590 (1985).
46. Shields, A. F. et al. Imaging proliferation in vivo with [F-18]FLT and positron emission tomography. *Nat. Med.* **4**, 1334–1336 (1998).
47. Abercrombie, M. Estimation of nuclear population from microtome sections. *Anat. Rec.* **94**, 239–247 (1946).

Acknowledgements We thank all of the patients who participated in this trial; Y. Shimizu, T. Saga and K. Togashi for brain imaging; members of the Efficacy and Safety Evaluation Committee, including S. Kinoshita, H. Sawada and H. Toda for their advice; doctors and coordinators at the Institute for Advancement of Clinical and Translational Science (iACT), Kyoto University Hospital, including A. Shimizu, Y. Nagai, M. Yamamoto, R. Uozumi, Y. Kusunoki, A. Kuroda, K. Endo, K. Enomoto, A. Kinoshita, C. Kimura, K. Kawaguchi, C. Ichihara, N. Matsuyama, K. Tochigi, Y. Sameshima, M. Iwasaki and C. Toyooka for supporting this clinical trial; the technical staff of J.T.'s laboratory, including E. Yamasaki, T. Ashida, Y. Fujita, Y. Tanikawa, Y. Katano, Y. Ozaki, R. Takaichi, A. Mihara, K. Fukushima and S. Baba for cell manufacturing; PD project members of Sumitomo Pharma, including K. Yoshida, H. Takahashi, Y. Sugao, S. Sekiya, M. Ikeda, Y. Yamamoto, S. Ota, S. Okabe, H. Ohara and T. Karino for regulatory support and cell manufacturing; and K. Hui for reading this manuscript. This study was supported by a grant from the Research Project for Practical Application of Regenerative Medicine of the Japan Agency for Medical Research and Development (AMED) (23bk0104126h0003) to J.T.

Author contributions J.T. and R.T. were the lead investigators. N.S., D.D. and Takayuki Kikuchi wrote the first draft of the paper. N.S., E.N., M.S., H.Y., Y.T., A.S., Y.F., T.O., Y.N. and R.T. contributed to the acquisition of clinical data. D.D., Tetsuhiro Kikuchi, A.M. and J.T. contributed to the generation of human iPSC cells and DA progenitor cells. S.H. contributed to the PD rat experiments. Takayuki Kikuchi, Y.A. and S. Miyamoto contributed to neurosurgery. T.A. and T.S. contributed to immunosuppressive therapy management. K.U. and S. Morita performed statistical analyses. All of the authors contributed to the analysis or interpretation of data and performed critical revisions of the manuscript.

Competing interests N.S., R.T. and J.T. received a grant for collaborative research from Sumitomo Pharma. R.T. received a research grant from Nihon Medi-Physics. T.O. received a research grant from Siemens Healthcare. S.H. is an employee of Sumitomo Pharma. The other authors declare no competing interests.

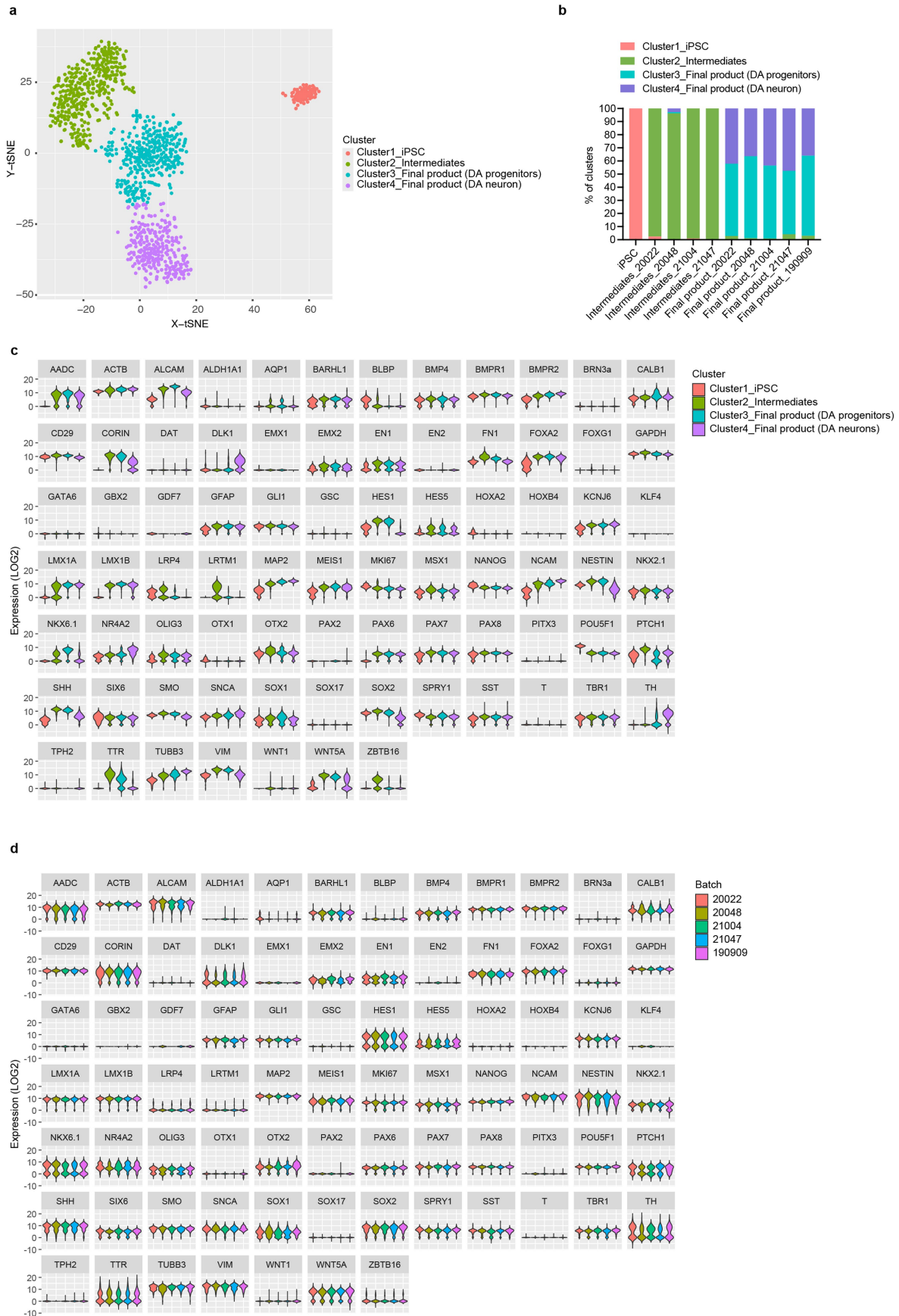
Additional information

Supplementary information The online version contains supplementary material available at <https://doi.org/10.1038/s41586-025-08700-0>.

Correspondence and requests for materials should be addressed to Ryosuke Takahashi or Jun Takahashi.

Peer review information Nature thanks David Devos, Hideyuki Okano and the other, anonymous, reviewer(s) for their contribution to the peer review of this work. Peer reviewer reports are available.

Reprints and permissions information is available at <http://www.nature.com/reprints>.

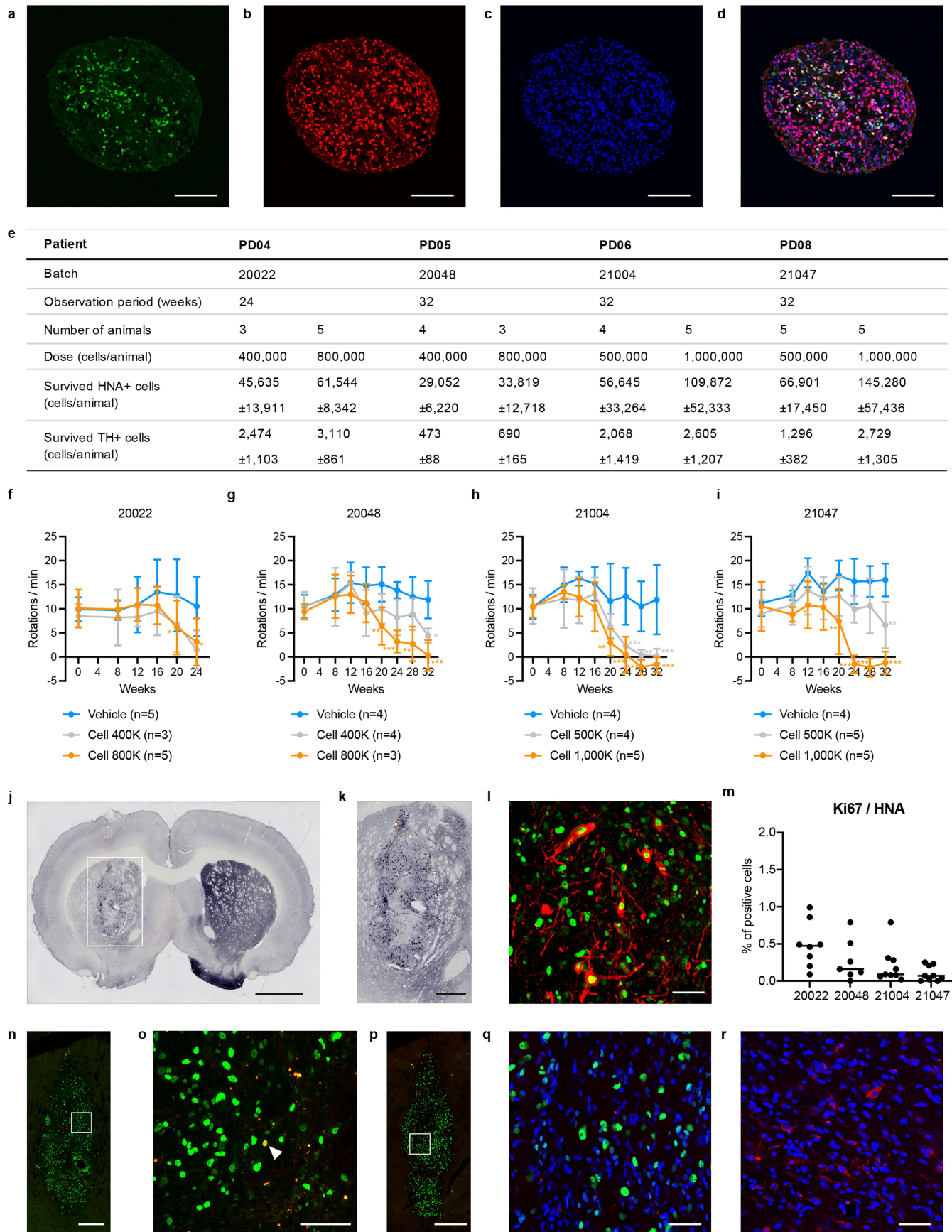


Extended Data Fig. 1 | See next page for caption.

Extended Data Fig. 1 | Single-cell RT-qPCR (sc-RT-qPCR) analysis of cells during DA differentiation. **a.** t-SNE plot of sc-RT-qPCR data for iPSCs, intermediate cells (before CORIN-positive cell sorting), and final products. iPSCs and intermediate cells each form a distinct cluster, while final products are divided into two clusters. **b.** Relative proportions of cell types in each cell sample, determined by K-means clustering of sc-RT-qPCR data, indicate the final product consists of approximately 60% DA progenitors and 40% DA

neurons. Batch #20022 was the donor cells used for PD04, Batch #20048 for PD05, Batch #21004 for PD06, and Batch #21047 for PD08. Batch #190909 was used for PD02. **c.** Violin plots of gene expression patterns in clusters of iPSCs, intermediate cells, and final products show gene expression changes during DA differentiation. **d.** Violin plots of gene expression patterns across different batches of final products indicate stable expression among batches.

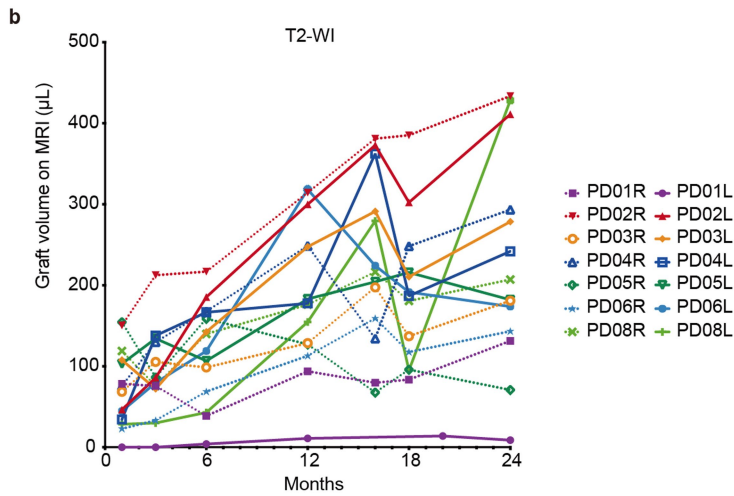
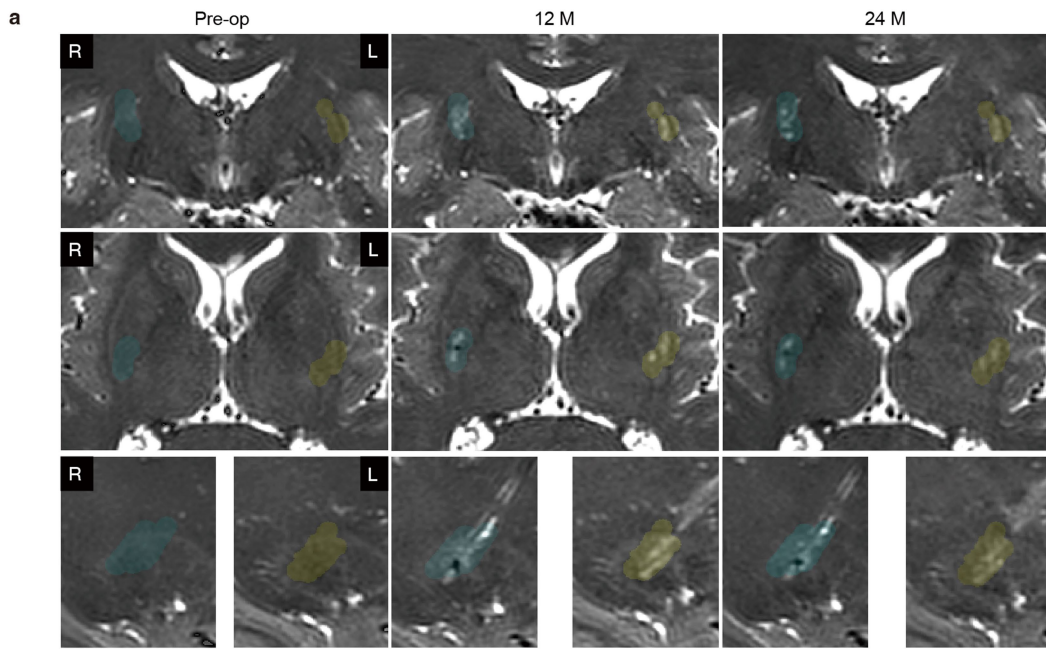
Article



Extended Data Fig. 2 | See next page for caption.

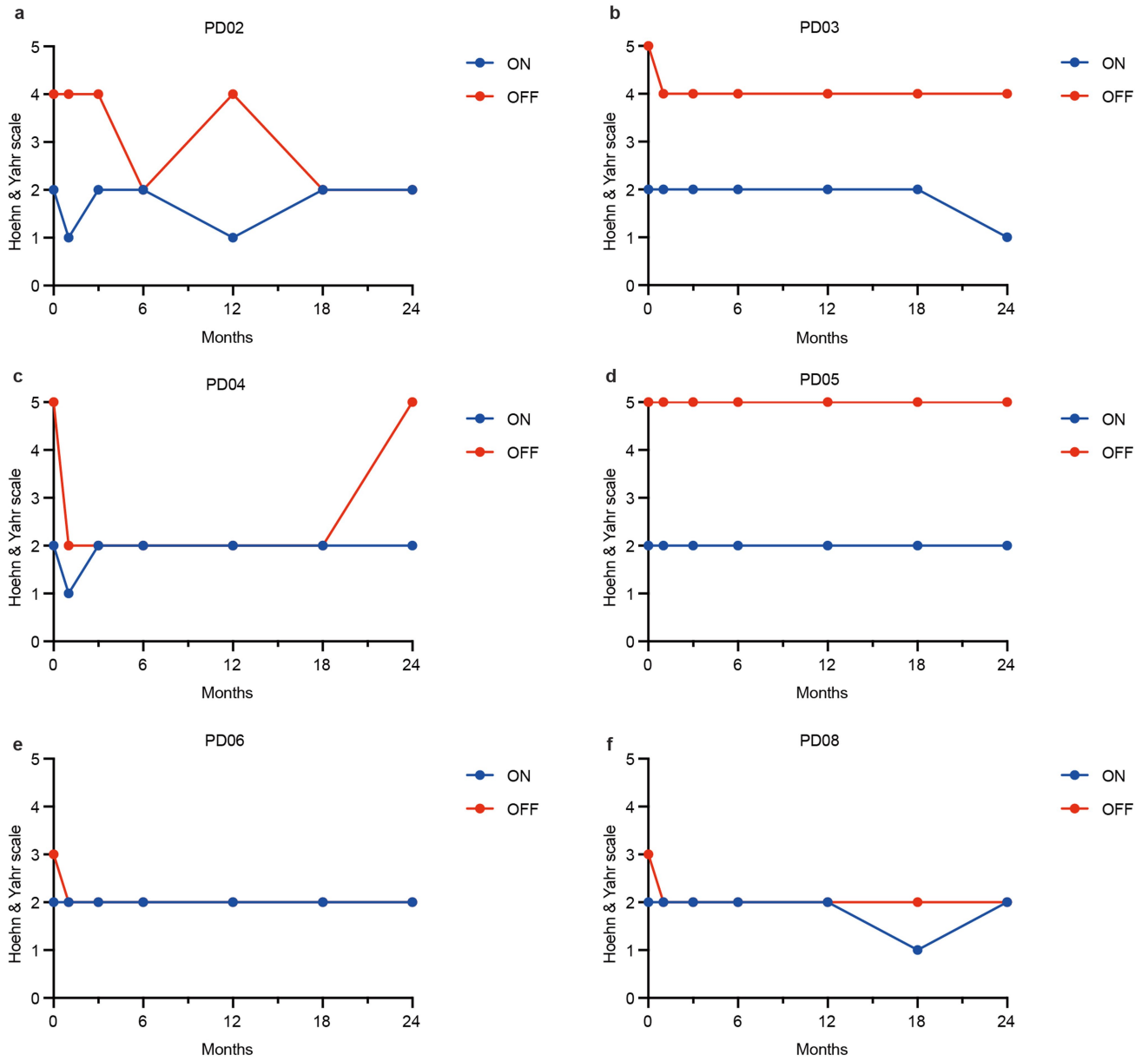
Extended Data Fig. 2 | Transplantation of the same donor cells used for patients into rat PD models. a-d. Immunofluorescence images of donor cells on day 30 (n = 7 independent experiments). NURR1 (a) is a nuclear receptor expressed in DA neurons, while FOXA2 (b) is a transcription factor expressed in the floor plate. DAPI (c) is used for nuclear staining. The merged image (d) shows that donor cells consist mainly of DA progenitors and some DA neurons. Scale bars = 100 μ m. e. Summary of cell transplantation experiments and results. Low- and high-dose cell injections were administered to examine differences in cell survival and behavioural improvement. f-i. Methamphetamine-induced rotation behaviour in rats with grafts shows improvement at approximately 24 weeks. Data are presented as mean \pm s.d. * p < 0.05, ** p < 0.01, *** p < 0.001 versus vehicle group by a two-way analysis of variance (ANOVA) with Tukey's multiple comparisons test. f. Adjusted p value = 0.033 (20 weeks) and 0.045 (24 weeks). g. Adjusted p value = 0.006 (20 weeks), <0.001 (24 weeks), 0.002 (28 weeks), 0.011 (32 weeks, Vehicle vs. Cell 400 K), and <0.001 (32 weeks, Vehicle vs. Cell 800 K). h. Adjusted p value = 0.004 (20 weeks), 0.001 (28 weeks, Vehicle vs. Cell 500 K), and the others <0.001. i. Adjusted p value = 0.033 (12 weeks), 0.001 (20 weeks), 0.002 (32 weeks, Vehicle vs. Cell 500 K), 0.006 (32 weeks, Vehicle vs. Cell 1,000 K), and the others <0.001. jk. DAB staining for TH

(tyrosine hydroxylase, a marker for DA neurons) in representative grafts at 32 weeks (n = 4 independent experiments). Scale bar = 2 mm. k. Magnified image of the graft shown in panel j. Scale bar = 500 μ m. l. Immunofluorescence image of the graft double-labelled for TH and HNA-positive cells indicating donor-derived DA neurons (n = 4 independent experiments). Scale bar = 50 μ m. m. Percentage of KI67-positive cells relative to HNA-positive cells for each graft. N = 8 (batch 20022), 7 (batch 20048), 9 (batch 21004), and 9 (batch 21047) biologically independent animals, respectively. Line = median. n. Immunofluorescence image of the graft stained for HNA (green) and KI67 (red), n = 4 independent experiments. Scale bar = 500 μ m. o. Magnified image of the graft shown in panel n, with an arrowhead indicating an HNA/KI67 double-positive cell. p. Immunofluorescence image of the graft stained for HNA (green) and 5-HT (red), n = 4 independent experiments. Scale bar = 500 μ m. q. Magnified image of the graft shown in panel p, showing the absence of HNA/5-HT double-positive cells. DAPI staining is shown in blue. Scale bar = 50 μ m. r. Immunofluorescence image of the host Raphe nucleus as a positive control for serotonergic neurons (5-HT, red) DAPI staining is shown in blue (n = 4 independent experiments). Scale bar = 50 μ m.



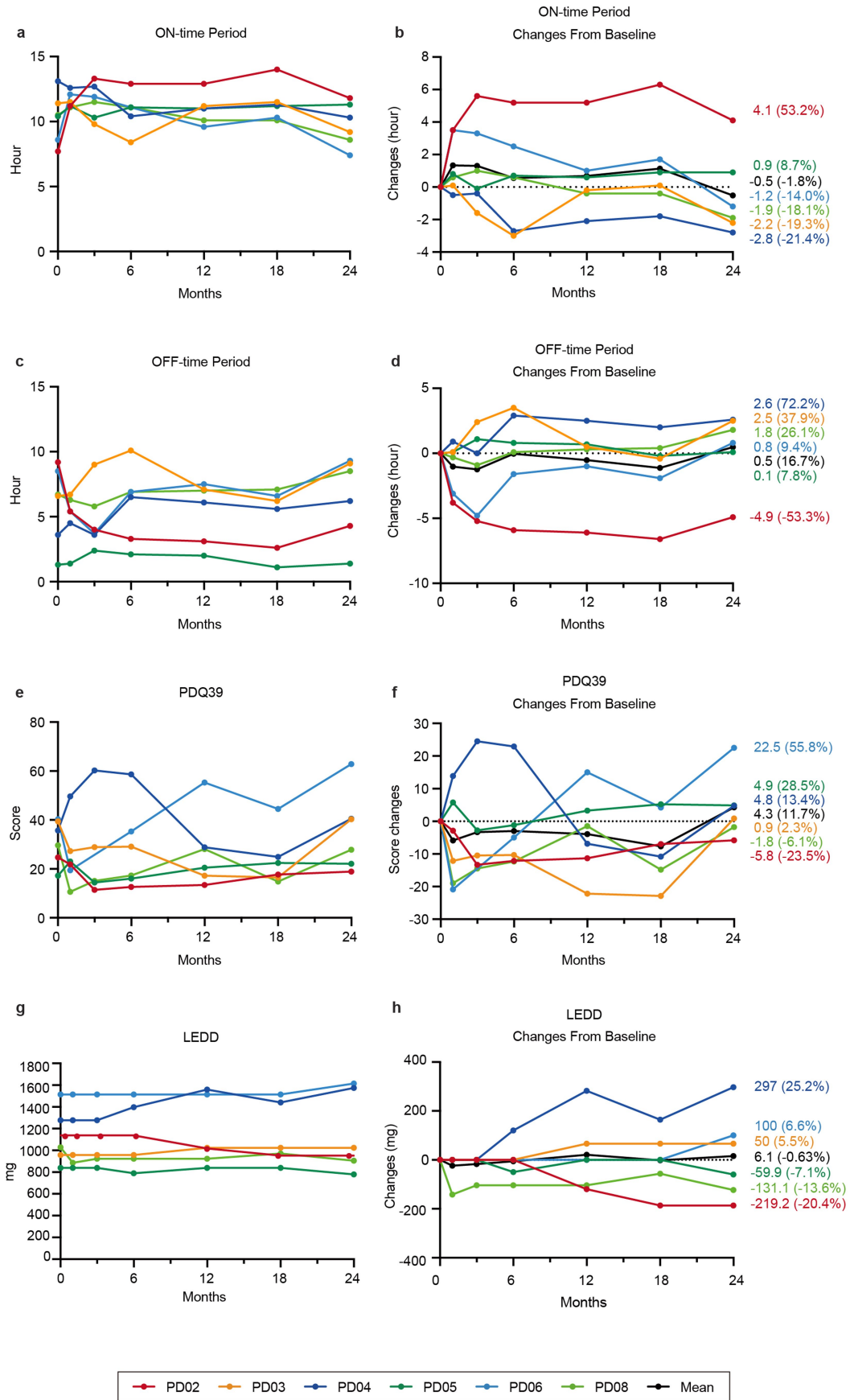
Extended Data Fig. 3 | Cell survival of iPSC-derived DA progenitors.
a. T2-weighted MR images of patient PD08, showing grafts as hyperintense areas. Coronal, axial, and sagittal images are displayed from top to bottom. Blue and yellow regions indicate areas within 3 mm of cell injection sites.

b. Changes in graft volume as measured by T2-weighted MR images of each patient. Hyperintense areas within the blue and yellow regions were calculated (R: right and L: left).



Extended Data Fig. 4 | Changes in the Hoehn and Yahr scale for each patient. The Hoehn and Yahr scale was evaluated at 3, 6, 12, 18, and 24 months. "ON" indicates measurements taken while the patient was on medication, while

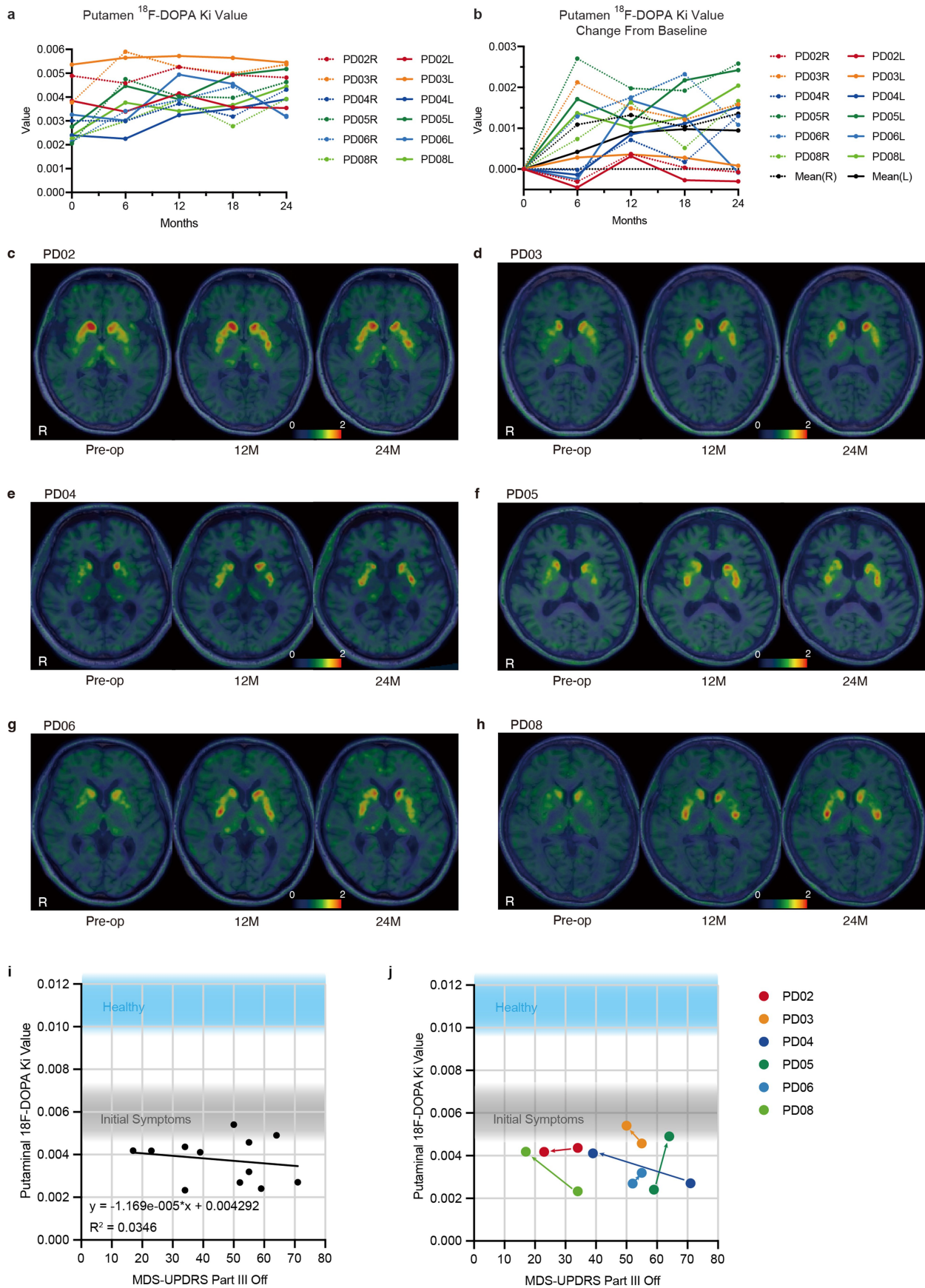
"OFF" indicates measurements taken after the patient had been off medication for more than 12 h.



Extended Data Fig. 5 | See next page for caption.

Extended Data Fig. 5 | Changes in ON-time, OFF-time, PDQ-39 scores, and changes in levodopa equivalent daily dose (LEDD) for each patient. **a-f**, Chronological changes in ON-time period, OFF-time period, and PDQ39 scores for each patient from registration (0 M) to the end of the observation period (24 M), respectively, based on the patient's subjective perception. **b,d,f**, Score changes from baseline, with the mean represented by the black line. Absolute and relative (percentage) changes at 24 months are shown on

the right. **g,h**, Changes in levodopa equivalent daily dose (LEDD) for each patient. Medication data for each patient was collected from medical charts, and LEDD was calculated according to a previously established method²⁰. **g**, Chronological changes in LEDD for each patient from registration (0 M) to the end of the observation period (24 M). **h**, Score changes from baseline, with the mean represented by the black line. Absolute and relative (percentage) changes at 24 months are shown on the right.



Extended Data Fig. 6 | See next page for caption.

Extended Data Fig. 6 | Dopamine synthesis detected by ^{18}F -DOPA PET.

a, Chronological changes in the fluorine-18-L-dihydroxyphenylalanine (^{18}F -DOPA) Ki values for each side of the putamen for each patient from registration (0 M) to the end of the observation period (24 M), as a supplement to Fig. 3. **b**, Changes in Ki values from baseline, with the mean represented by the black line.

c-h, semiquantitative ^{18}F -DOPA images generated at 80–90 min post-injection by subtracting the occipital background signal and normalizing the result to the occipital activity for each patient (Pre-Op: pre-operation, 12 M: 12 months, 24 M: 24 months). The colour change from dark green to red in the bilateral

putamen indicates increased ^{18}F -DOPA uptake, reflecting dopamine synthesis by grafted cells. **i, j**, Relationship between ^{18}F -DOPA uptake and motor symptom improvement. **(i)** Plots of pre- and post-transplant Ki values and MDS-UPDRS part III OFF scores for six (PD02-08) patients. Healthy and initial symptom ranges are indicated based on previous studies, where Ki values for healthy individuals range from 0.010 to 0.017, and initial Parkinsonian symptoms emerge with Ki values between 0.0045 and 0.0073. **(j)** Changes in Ki values and MDS-UPDRS part III OFF scores for each patient.

Article

Extended Data Table 1 | Clinical characteristics of the participants at baseline

| | Low-dose subgroup | | | High-dose subgroup | | | |
|-----------------------------|-------------------|------|------|--------------------|------|------|------|
| | PD01 | PD02 | PD03 | PD04 | PD05 | PD06 | PD08 |
| Age (years) | 50 | 62 | 60 | 61 | 69 | 58 | 56 |
| Sex (F/M) | M | F | F | M | M | M | F |
| Duration (years) | 10.3 | 8.8 | 9.5 | 10.3 | 8.7 | 12.2 | 9.5 |
| Motor fluctuations | Yes | Yes | Yes | Yes | Yes | Yes | Yes |
| Hoehn & Yahr OFF | 3 | 4 | 5 | 5 | 5 | 3 | 3 |
| Hoehn & Yahr ON | 2 | 2 | 2 | 2 | 2 | 2 | 2 |
| Levodopa response (%) | 69.7 | 89.7 | 67.3 | 57.4 | 75.8 | 68.0 | 67.0 |
| Dyskinesia | Mild | None | Mild | Mild | Mild | Mild | Mild |
| HLA-matched (6 alleles*) | Yes | No | No | Yes | No | Yes | No |

Patients are subdivided into Low- and High-dose groups, and clinical characteristics at registration are presented. * Donor HLA-A 24:02, HLA-B 52:01, HLA-DRB1 15:02, HLA-C 12:02, HLA-DQB1 06:01, HLA-DPB1 09:01.

Extended Data Table 2 | Core clinical measures at 0 and 24 months after bilateral transplantation

| End Point | Low-dose subgroup (N = 2) | | | High-dose subgroup (N = 4) | | | Total (N = 6) | | |
|---|---------------------------|--------------------|------------------|----------------------------|---------------------|------------------|---------------------|---------------------|------------------|
| | 0M (SD) | 24M (SD) | % change (SD) | 0M (SD) | 24M (SD) | % change (SD) | 0M (SD) | 24M (SD) | % change (SD) |
| UDysRS (total)* | 7.7 (4.0) | 22.0 (5.6) | 219.4 (97.3) | 31.0 (8.6) | 41.8 (7.8) | 39.2 (28.0) | 21.0 (14.1) | 33.3 (12.3) | 116.4 (113.3) |
| MDS-UPDRS III OFF | 44.5 (14.8) | 36.5 (19.1) | -20.7 (16.4) | 54.0 (15.5) | 43.8 (20.6) | -20.2 (31.6) | 50.8 (14.6) | 41.3 (18.5) | -20.4 (25.6) |
| MDS-UPDRS III ON | 10.5 (3.5) | 4.5 (0.7) | -53.4 (22.4) | 21.3 (7.7) | 17.8 (13.4) | -26.8 (47.1) | 17.7 (8.3) | 13.3 (12.4) | -35.7 (40.2) |
| MDS-UPDRS II | 14.0 (4.2) | 14.0 (5.7) | -1.6 (10.6) | 8.3 (4.3) | 16.5 (7.2) | 127.0 (129.3) | 10.2 (4.9) | 15.7 (6.3) | 84.1 (120.2) |
| MDS-UPDRS I | 7.0 (0.0) | 7.0 (1.4) | 0.0 (20.2) | 4.5 (2.6) | 5.8 (4.0) | 19.0 (22.3) | 5.3 (2.4) | 6.2 (3.3) | 12.7 (21.9) |
| Bradykinesia subscale | 17.0 (4.2) | 12.5 (5.0) | -27.9 (11.1) | 17.8 (5.0) | 16.8 (7.4) | -7.0 (33.7) | 17.5 (4.3) | 15.3 (6.5) | -14.0 (28.7) |
| Hoehn & Yahr OFF | 4.5 (0.7) | 3.0 (1.4) | -35.0 (21.2) | 4.0 (1.2) | 3.5 (1.7) | -16.7 (19.2) | 4.2 (1.0) | 3.3 (1.5) | -22.8 (20.0) |
| Hoehn & Yahr ON | 2.0 (0.0) | 1.5 (0.7) | -25.0 (35.4) | 2.0 (0.0) | 2.0 (0.0) | 0.0 (0.0) | 2.0 (0.0) | 1.8 (0.4) | -8.3 (20.4) |
| OFF time without dyskinesia (hrs.) | 7.93 (1.82) | 6.61 (3.38) | -9.4 (63.5) | 4.63 (3.45) | 5.89 (3.83) | 34.1 (65.8) | 5.73 (3.27) | 6.13 (3.35) | 19.6 (62.5) |
| OFF time with non-troublesome dyskinesia (hrs.) | 0.00 (0.00) | 0.07 (0.00) | - | 0.30 (0.52) | 0.27 (0.54) | -50.0 (70.7) | 0.20 (0.43) | 0.20 (0.43) | -50.0 (70.7) |
| OFF time with troublesome dyskinesia (hrs.) | 0.00 (0.00) | 0.00 (0.00) | - | 0.09 (0.18) | 0.20 (0.24) | -20.0 (-) | 0.06 (0.15) | 0.13 (0.21) | -20.0 (-) |
| ON time without dyskinesia (hrs.) | 9.57 (2.63) | 9.86 (1.31) | 9.0 (43.6) | 7.86 (0.35) | 6.05 (3.56) | -21.7 (48.6) | 8.43 (1.50) | 7.32 (3.44) | -11.5 (45.3) |
| ON time with non-troublesome dyskinesia (hrs.) | 0.00 (0.00) | 0.36 (0.10) | - | 2.34 (1.97) | 1.48 (1.22) | -30.4 (18.5) | 1.56 (1.94) | 1.11 (1.11) | -30.4 (18.5) |
| ON time with troublesome dyskinesia (hrs.) | 0.00 (0.00) | 0.29 (0.40) | - | 0.43 (0.43) | 1.86 (2.78) | 318.3 (338.1) | 0.29 (0.40) | 1.33 (2.31) | 318.3 (338.1) |
| PDQ-39 (Summary Index) | 32.08 (10.39) | 29.58 (15.10) | -10.7 (18.2) | 30.69 (10.02) | 38.31 (18.02) | 23.0 (26.0) | 31.15 (9.07) | 35.40 (16.15) | 11.8 (27.9) |
| LEDD (mg/day)** | 990.00 (115.82) | 905.40 (74.53) | -7.47 (18.36) | 1123.10 (295.73) | 1174.61 (431.10) | 2.76 (17.19) | 1078.73 (244.70) | 1084.88 (363.25) | -0.65 (16.51) |
| ¹⁸ F-DOPA putamen Ki | 0.0045 (0.0001) | 0.0048 (0.0009) | 7.0 (15.9) | 0.0025 (0.0002) | 0.0041 (0.0007) | 63.5 (36.8) | 0.0032 (0.0010) | 0.0043 (0.0008) | 44.7 (41.4) |
| ¹⁸ F-DOPA caudate Ki | 0.0090 (0.0007) | 0.0084 (0.0001) | -6.9 (6.8) | 0.0068 (0.0004) | 0.0068 (0.0001) | 0.3 (4.8) | 0.0076 (0.0012) | 0.0073 (0.0008) | -2.1 (6.0) |

Core clinical measures at registration (0M) and the end of observation (24M) are presented by mean and standard deviation (SD, in parentheses). * The UDysRS is included in the safety profile, and results are presented for the safety population [Low-dose (N=3), High-dose (N=4), and total (N=7)]. In PD01, the right-side transplantation was performed 8 months after the initial left-side transplantation. Therefore, the assessment interval from the preoperative period to 24 months post-bilateral transplantation was 32 months. ** This LEDD was calculated using an updated formula published after the trial's initiation²¹. Although the average score increased, the percentage change decreased. For completeness, we have retained the data calculated using an older formula in Extended Data Fig. 5g,h²⁰. LEDD, Levodopa equivalent daily dose; MDS-UPDRS, Movement Disorder Society Unified Parkinson's disease Rating Scale; OFF, drug-off state; ON, drug-on state; PDQ-39, 39-item Parkinson's Disease Questionnaire; UDysRS, Unified Dyskinesia Rating Scale.

Article

Extended Data Table 3 | Additional clinical measures at 0 and 24 months after bilateral transplantation

| End Point | Low dose (N = 2) | | | High dose (N = 4) | | | Total (N = 6) | | |
|-----------------------------------|------------------|------------------|------------------|-------------------|------------------|------------------|------------------|------------------|------------------|
| | 0M (SD) | 24M (SD) | % change (SD) | 0M (SD) | 24M (SD) | % change (SD) | 0M (SD) | 24M (SD) | % change (SD) |
| MDS-UPDRS | | | | | | | | | |
| Total of parts I, II, and III OFF | 65.5 (19.1) | 57.5 (26.2) | -14.4 (15.0) | 66.8 (17.7) | 66.0 (24.9) | -3.6 (22.0) | 66.3 (16.2) | 63.2 (23.0) | -7.2 (19.1) |
| Total of parts I, II, and III ON | 31.5 (7.8) | 25.5 (6.4) | -19.1 (0.2) | 34.0 (11.4) | 40.0 (19.0) | 11.9 (25.1) | 33.2 (9.6) | 35.2 (16.8) | 1.6 (25.2) |
| EQ-5D-5L | | | | | | | | | |
| Index score | 0.66 (0.10) | 0.75 (0.20) | 13.4 (13.3) | 0.61 (0.33) | 0.60 (0.29) | 13.1 (49.1) | 0.62 (0.26) | 0.65 (0.26) | 13.2 (38.5) |
| EQ VAS | 75.00 (7.07) | 82.50 (10.61) | 9.8 (3.8) | 55.0 (24.83) | 60.00 (26.77) | 34.8 (113.2) | 61.67 (22.06) | 67.50 (24.24) | 26.5 (88.7) |
| WPAI | | | | | | | | | |
| Absenteeism | 0 | 0 | 0 | 0 | 0 | 0 | 0 | 0 | 0 |
| Presenteeism | 0 | 0 | 0 | 0 | 0 | 0 | 0 | 0 | 0 |
| Overall work impairment | 0 | 0 | 0 | 0 | 0 | 0 | 0 | 0 | 0 |
| Activity impairment | 55.00 (35.36) | 55.00 (35.36) | 0.0 (0.0) | 50.00 (39.16) | 57.50 (38.62) | 11.7 (97.9) | 51.67 (34.30) | 56.67 (33.86) | 7.8 (76.1) |

Core clinical measures at registration (0M) and the end of observation (24M) are presented by mean and SD (in parentheses). EQ-5D-5L, EuroQol 5-dimension 5-level, [European Quality of life-5 dimensions questionnaire (EQ-5D)]; EQ VAS, EuroQol Visual Analogue Scale; WPAI, Work Productivity and Activity Impairment.

Reporting Summary

Nature Portfolio wishes to improve the reproducibility of the work that we publish. This form provides structure for consistency and transparency in reporting. For further information on Nature Portfolio policies, see our [Editorial Policies](#) and the [Editorial Policy Checklist](#).

Statistics

For all statistical analyses, confirm that the following items are present in the figure legend, table legend, main text, or Methods section.

- | n/a | Confirmed |
|-------------------------------------|--|
| <input type="checkbox"/> | <input checked="" type="checkbox"/> The exact sample size (n) for each experimental group/condition, given as a discrete number and unit of measurement |
| <input type="checkbox"/> | <input checked="" type="checkbox"/> A statement on whether measurements were taken from distinct samples or whether the same sample was measured repeatedly |
| <input type="checkbox"/> | <input checked="" type="checkbox"/> The statistical test(s) used AND whether they are one- or two-sided <i>Only common tests should be described solely by name; describe more complex techniques in the Methods section.</i> |
| <input checked="" type="checkbox"/> | <input type="checkbox"/> A description of all covariates tested |
| <input checked="" type="checkbox"/> | <input type="checkbox"/> A description of any assumptions or corrections, such as tests of normality and adjustment for multiple comparisons |
| <input type="checkbox"/> | <input checked="" type="checkbox"/> A full description of the statistical parameters including central tendency (e.g. means) or other basic estimates (e.g. regression coefficient) AND variation (e.g. standard deviation) or associated estimates of uncertainty (e.g. confidence intervals) |
| <input type="checkbox"/> | <input checked="" type="checkbox"/> For null hypothesis testing, the test statistic (e.g. F , t , r) with confidence intervals, effect sizes, degrees of freedom and P value noted <i>Give P values as exact values whenever suitable.</i> |
| <input checked="" type="checkbox"/> | <input type="checkbox"/> For Bayesian analysis, information on the choice of priors and Markov chain Monte Carlo settings |
| <input checked="" type="checkbox"/> | <input type="checkbox"/> For hierarchical and complex designs, identification of the appropriate level for tests and full reporting of outcomes |
| <input checked="" type="checkbox"/> | <input type="checkbox"/> Estimates of effect sizes (e.g. Cohen's d , Pearson's r), indicating how they were calculated |

Our web collection on [statistics for biologists](#) contains articles on many of the points above.

Software and code

Policy information about [availability of computer code](#)

Data collection EDMS-Online ver.3.1

Data analysis Brain images were processed using Functional Magnetic Resonance Imaging of the Brain (fMRIB) Software Library (FSL 5.3) and Statistical Parametric Mapping 12 (SPM12, Release 7219). Statistical analyses of clinical data were conducted using SAS software (version 9.4, SAS Institute), and statistical analysis of animal experiments were performed using GraphPad Prism (version 10.3.1, GraphPad Software).

For manuscripts utilizing custom algorithms or software that are central to the research but not yet described in published literature, software must be made available to editors and reviewers. We strongly encourage code deposition in a community repository (e.g. GitHub). See the Nature Portfolio [guidelines for submitting code & software](#) for further information.

Data

Policy information about [availability of data](#)

All manuscripts must include a [data availability statement](#). This statement should provide the following information, where applicable:

- Accession codes, unique identifiers, or web links for publicly available datasets
- A description of any restrictions on data availability
- For clinical datasets or third party data, please ensure that the statement adheres to our [policy](#)

All relevant data from this trial are included in the article and Supplementary Material.

Research involving human participants, their data, or biological material

Policy information about studies with [human participants or human data](#). See also policy information about [sex, gender \(identity/presentation\), and sexual orientation](#) and [race, ethnicity and racism](#).

| | |
|--|---|
| Reporting on sex and gender | Participants were enrolled irrespective of their sex. Data are provided in Extended Data Table 1. |
| Reporting on race, ethnicity, or other socially relevant groupings | Participants were enrolled irrespective of their race/ethnicity. |
| Population characteristics | Data are provided in Extended Data Table 1 |
| Recruitment | A public call was made by website, press conference. Patients were selected from among those who wished to participate, after consultation by a selection committee in accordance with the selection criteria. Potential biases (placebo effect and observer bias) are noted in the discussion. |
| Ethics oversight | The protocol was reviewed and approved by Kyoto University Hospital Institutional Review Board (K044). |

Note that full information on the approval of the study protocol must also be provided in the manuscript.

Field-specific reporting

Please select the one below that is the best fit for your research. If you are not sure, read the appropriate sections before making your selection.

Life sciences Behavioural & social sciences Ecological, evolutionary & environmental sciences

For a reference copy of the document with all sections, see [nature.com/documents/nr-reporting-summary-flat.pdf](https://www.nature.com/documents/nr-reporting-summary-flat.pdf)

Life sciences study design

All studies must disclose on these points even when the disclosure is negative.

| | |
|-----------------|---|
| Sample size | Based on the results of the monkey study (Kikuchi et al Nature 2017), we calculated number of samples for which safety could be assessed. Details are given in the Statistic Analysis Plan p 3. "Target sample size". |
| Data exclusions | No data were excluded. |
| Replication | We replicated the transplantation of iPSC-derived dopaminergic progenitors in a total of 7 participants. We confirmed all attempts were successful. |
| Randomization | This trial was not randomized. When selecting patients, the male/female ratio (4:3) and HLA match or incompatibility (3:4) were not biased among patients who met the selection criteria. |
| Blinding | This trial was a single-arm trial. |

Reporting for specific materials, systems and methods

We require information from authors about some types of materials, experimental systems and methods used in many studies. Here, indicate whether each material, system or method listed is relevant to your study. If you are not sure if a list item applies to your research, read the appropriate section before selecting a response.

Materials & experimental systems

| n/a | Involvement in the study |
|-------------------------------------|---|
| <input type="checkbox"/> | <input checked="" type="checkbox"/> Antibodies |
| <input type="checkbox"/> | <input checked="" type="checkbox"/> Eukaryotic cell lines |
| <input checked="" type="checkbox"/> | <input type="checkbox"/> Palaeontology and archaeology |
| <input type="checkbox"/> | <input checked="" type="checkbox"/> Animals and other organisms |
| <input type="checkbox"/> | <input checked="" type="checkbox"/> Clinical data |
| <input checked="" type="checkbox"/> | <input type="checkbox"/> Dual use research of concern |
| <input checked="" type="checkbox"/> | <input type="checkbox"/> Plants |

Methods

| n/a | Involvement in the study |
|-------------------------------------|--|
| <input checked="" type="checkbox"/> | <input type="checkbox"/> ChIP-seq |
| <input checked="" type="checkbox"/> | <input type="checkbox"/> Flow cytometry |
| <input type="checkbox"/> | <input checked="" type="checkbox"/> MRI-based neuroimaging |

Antibodies

| | |
|-----------------|--|
| Antibodies used | Primary antibodies used are as follows: FOXA2 (goat, R&D systems, AF2400, 1:500), NURR1 (mouse, Perseus Proteomics, PP-N1404-00, 1:300), HNA (mouse, Millipore, MAB1281, 1:500, KI67 (rabbit, Abcam, Ab16667, 1:1,000), 5-HT (rat, Millipore MAB352, 1:100), and TH (rabbit, Millipore, AB152, 1:400). Secondary antibodies are as follows: Alexa Fluor 488 anti-Mouse IgG, (donkey, ThermoFisher, A21202, 1:400), Alexa Fluor 594 anti-Goat IgG (donkey, ThermoFisher, A11058, 1:2,000), Alexa Fluor 594 anti-Rabbit IgG (donkey, ThermoFisher, A21207, 1:400), and Alexa Fluor 594 anti-Rat IgG (donkey, ThermoFisher, A21209, 1:400). |
| Validation | Antibodies are used under validation using adequate negative and positive control samples. We confirmed the staining by using animal samples when possible, or we rely on the stained samples presented in manufacturer's website (FOXA2 from R&D, HNA from Millipore, KI67 from Abcam, and 5-HT and TH from Millipore). |

Eukaryotic cell lines

Policy information about [cell lines and Sex and Gender in Research](#)

| | |
|---|---|
| Cell line source(s) | iPSCs are derived from human peripheral blood cells, donated by healthy volunteer. QHJIO1s04 is provided by Center for iPS cell Research and Application (CiRA), Kyoto University, Japan. MCB003 is provided by Sumitomo Pharma (Tokyo, Japan). |
| Authentication | The STR (short tandem repeat) pattern of iPSCs coincide with that of donor cells. |
| Mycoplasma contamination | All cells are negative for mycoplasma contamination. |
| Commonly misidentified lines (See ICLAC register) | Nothing. |

Animals and other research organisms

Policy information about [studies involving animals; ARRIVE guidelines](#) recommended for reporting animal research, and [Sex and Gender in Research](#)

| | |
|-------------------------|--|
| Laboratory animals | Adult (9-week-old) male nude rats (F344/NJcl-rnu/rnu, CLEA, Japan) were used for this study. |
| Wild animals | The study did not involve wild animals. |
| Reporting on sex | In this study, only male rats were used to precisely examine the effect of transplanted cells by excluding effects of the female's sexual cycle on the survival or maturation of dopaminergic neurons. |
| Field-collected samples | The study did not involve samples collected from the field. |
| Ethics oversight | The study protocol is approved by the ethical committees of Kyoto University and Sumitomo Pharma. |

Note that full information on the approval of the study protocol must also be provided in the manuscript.

Clinical data

Policy information about [clinical studies](#)

All manuscripts should comply with the ICMJE [guidelines for publication of clinical research](#) and a completed [CONSORT checklist](#) must be included with all submissions.

| | |
|-----------------------------|--|
| Clinical trial registration | jRCT2090220384, UMIN000033564 |
| Study protocol | The study protocol was provided in the supplementary material. |
| Data collection | This trial was conducted at Kyoto University Hospital. Patients are recruited from Aug. 1, 2018 to May 19, 2021. Data are collected from Sep. 25, 2018 to Jan. 18, 2024. |
| Outcomes | Primary end points included the adverse-event profile and secondary end points involved the safety and efficacy at 24 months |

Plants

| | |
|-----------------------|---|
| Seed stocks | Report on the source of all seed stocks or other plant material used. If applicable, state the seed stock centre and catalogue number. If plant specimens were collected from the field, describe the collection location, date and sampling procedures. |
| Novel plant genotypes | Describe the methods by which all novel plant genotypes were produced. This includes those generated by transgenic approaches, gene editing, chemical/radiation-based mutagenesis and hybridization. For transgenic lines, describe the transformation method, the number of independent lines analyzed and the generation upon which experiments were performed. For gene-edited lines, describe the editor used, the endogenous sequence targeted for editing, the targeting guide RNA sequence (if applicable) and how the editor was applied. |
| Authentication | Describe any authentication procedures for each seed stock used or novel genotype generated. Describe any experiments used to assess the effect of a mutation and, where applicable, how potential secondary effects (e.g. second site T-DNA insertions, mosaicism, off-target gene editing) were examined. |

Magnetic resonance imaging

Experimental design

| | |
|---------------------------------|-----------------------------|
| Design type | This was not an fMRI study. |
| Design specifications | This was not an fMRI study. |
| Behavioral performance measures | This was not an fMRI study. |

Acquisition

| | |
|-------------------------------|--|
| Imaging type(s) | T1-weighted, T2-weighted, fluid-attenuated inversion recovery (FLAIR), and T2*-weighted images |
| Field strength | 3 Tesla scanner |
| Sequence & imaging parameters | Whole brain |
| Area of acquisition | State whether a whole brain scan was used OR define the area of acquisition, describing how the region was determined. |
| Diffusion MRI | <input type="checkbox"/> Used <input checked="" type="checkbox"/> Not used |

Preprocessing

| | |
|----------------------------|---|
| Preprocessing software | Functional Magnetic Resonance Imaging of the Brain (FMRIB) software |
| Normalization | Normalization was not conducted. |
| Normalization template | Not applicable |
| Noise and artifact removal | Not applicable |
| Volume censoring | Not applicable |

Statistical modeling & inference

| | |
|---|---|
| Model type and settings | Not applicable |
| Effect(s) tested | Not applicable |
| Specify type of analysis: | <input type="checkbox"/> Whole brain <input type="checkbox"/> ROI-based <input type="checkbox"/> Both |
| Statistic type for inference | Not applicable |
| (See Eklund et al. 2016) | |
| Correction | Not applicable |

Models & analysis

- n/a | Involved in the study
- Functional and/or effective connectivity
- Graph analysis
- Multivariate modeling or predictive analysis

Functional and/or effective connectivity

Report the measures of dependence used and the model details (e.g. Pearson correlation, partial correlation, mutual information).

Graph analysis

Report the dependent variable and connectivity measure, specifying weighted graph or binarized graph, subject- or group-level, and the global and/or node summaries used (e.g. clustering coefficient, efficiency, etc.).

Multivariate modeling and predictive analysis

Specify independent variables, features extraction and dimension reduction, model, training and evaluation metrics.